Disruption of bacterial interactions and community assembly in Babesia-infected Haemaphysalis longicornis following antibiotic treatment

Myriam Kratou, Apolline Maitre, Lianet Abuin-Denis, Elianne Piloto-Sardiñas, Ivan Corona-Guerrero, Ana Laura Cano-Argüelles, Alejandra Wu-Chuang, Timothy Bamgbose, Consuelo Almazan, Juan Mosqueda, et al.

BMC Microbiology

RESEARCH

Open Access

Disruption of bacterial interactions and community assembly in *Babesia*-infected *Haemaphysalis longicornis* following antibiotic treatment

Myriam Kratou[1*], Apolline Maitre[2,3,4], Lianet Abuin-Denis[2,5], Elianne Piloto-Sardiñas[2,6], Ivan Corona-Guerrero[7,8], Ana Laura Cano-Argüelles[9], Alejandra Wu-Chuang[2], Timothy Bamgbose[10,11], Consuelo Almazan[7,8], Juan Mosqueda[7,8], Dasiel Obregón[12], Lourdes Mateos-Hernández[2], Mourad Ben Said[1,13] and Alejandro Cabezas-Cruz[2*]

Abstract

Background A previous study highlighted the role of antibiotic-induced dysbiosis in the tick microbiota, facilitating the transstadial transmission of *Babesia microti* from nymph to adult in *Haemaphysalis longicornis*. This study builds on previous findings by analyzing sequence data from an earlier study to investigate bacterial interactions that could be linked to enhanced transstadial transmission of *Babesia* in ticks. The study employed antibiotic-treated (AT) and control-treated (CT) *Haemaphysalis longicornis* ticks to investigate shifts in microbial community assembly. Network analysis techniques were utilized to assess bacterial interactions, comparing network centrality measures between AT and CT groups, alongside studying network robustness and connectivity loss. Additionally, functional profiling was conducted to evaluate metabolic diversity in response to antibiotic treatment.

Results The analysis revealed notable changes in microbial community assembly in response to antibiotic treatment. Antibiotic-treated (AT) ticks displayed a greater number of connected nodes but fewer correlations compared to control-treated (CT) ticks, indicating a less interactive yet more connected microbial community. Network centrality measures such as degree, betweenness, closeness, and eigenvector centrality, differed significantly between AT and CT groups, suggesting alterations in local network dynamics due to antibiotic intervention. *Coxiella* and *Acinetobacter* exhibited disrupted connectivity and roles, with the former showing reduced interactions in AT group and the latter displaying a loss of connected nodes, emphasizing their crucial roles in microbial network stability. Robustness tests against node removal showed decreased stability in AT networks, particularly under directed attacks, confirming a susceptibility of the microbial community to disturbances. Functional profile analysis further indicated a higher diversity and richness in metabolic capabilities in the AT group, reflecting potential shifts in microbial metabolism as a consequence of antimicrobial treatment.

*Correspondence:
Myriam Kratou
mariem.kratou@hotmail.com
Alejandro Cabezas-Cruz
alejandro.cabezas@vet-alfort.fr
Full list of author information is available at the end of the article

Conclusions Our findings support that bacterial interaction traits boosting the transstadial transmission of *Babesia* could be associated with reduced colonization resistance. The disrupted microbial interactions and decreased network robustness in AT ticks suggest critical vulnerabilities that could be targeted for managing tick-borne diseases.

Keywords *Haemaphysalis longicornis*, *Babesia microti*, Microbiota, Microbial community assembly, Network analysis

Background

Ticks are obligate hematophagous arthropods that play a significant role in the transmission of various infectious agents, such as bacteria (e.g., *Borrelia* and *Anaplasma*), viruses (e.g., tick-borne encephalitis virus, TBEV), and protozoan parasites (e.g., *Babesia* and *Theileria*) [1]. The Asian long-horned tick, *Haemaphysalis longicornis*, has been associated with more than 30 human and animal pathogens, raising medical and veterinary concerns [2]. Originating from Eastern Asia, this tick has the capability to rapidly spread into new areas, presenting an emerging disease threat (e.g., recent invasion of USA) [2]. Notably, *H. longicornis* has been identified as a vector for *Babesia* [3]. Among *Babesia* pathogenic species, *B. microti* has gained significant recognition as the primary etiological agent responsible for babesiosis in humans, particularly in the USA [4, 5]. This hemoparasite can infect small rodents like mice and voles, serving as the primary reservoir hosts for *B. microti*.

The typical mode of *Babesia* transmission involves transovarial transmission through adult tick to their offspring [6, 7]. Transovarial transmission enhances species diversification by facilitating host switching to other vertebrate hosts [8]. In addition to transovarial transmission, *Babesia* pathogens exhibit transstadial transmission [9]. However, transovarial transmission of *B. microti* has been found absent in ticks belonging to the genus *Ixodes*, including *Ixodes ricinus* [10] as well as in ticks outside the *Ixodes* genus, such as *Rhipicephalus haemaphysalis* [11]. Consequently, this pathogen relies exclusively on transstadial transmission after acquisition from an infected host [10]. Furthermore, Gray et al. [10] experimentally demonstrated that while transstadial transmission occurs, the parasite does not persist after molting.

Combination therapies, typically involving an antiprotozoal agent and an antibiotic, were recommended and applied for the treatment of human babesiosis [12]. Antibiotics ingested with the tick's blood meal have the potential to disrupt the tick microbiota, leading to tick gut dysbiosis [5]. Ticks harbor a range of pathogenic microorganisms alongside endosymbionts and commensals, emphasizing the impact of these microbes on tick fitness and pathogen transmission [13, 14]. Microbiota dysbiosis may either reduce [15] or increase [16] the tick's susceptibility to tick-borne pathogens (TBPs), potentially shaping tick-borne diseases (TBDs) ecology. In the context of *B. microti*, gut microbiota has been found to play a role in facilitating the transstadial transmission of this pathogen from nymphs to adult *H. longicornis* ticks [16]. Furthermore, in their study, Wei et al. [16] found that antibiotics administered to mouse hosts altered the microbiota of adult ticks, with significant differences in the abundance of *Coxiella* and *Acinetobacter* between the antibiotic-treated group (AT) and the untreated control group (CT). *Coxiella* was the most abundant genus in CT adults, whereas *Acinetobacter* dominated in AT adults, indicating a shift in the microbiota composition due to antibiotics [16]. Similar evidence has been observed in *Plasmodium falciparum* parasites, where antibiotics have been shown to increase parasite colonization in mosquitoes [17], an effect mediated by the vector microbiota [17]. This highlights the significance of tick-microbiota interactions for vector competence, including the modulation of tick vector capacity by influencing pathogen colonization of tick tissues [18]. Overall, the evidence suggests a potential role of colonization resistance in the context of TBPs [19] where the microbiota within ticks may resist the colonization or transmission of TBPs like *B. microti* [16], a protection disrupted by antibiotic-induced dysbiosis [20].

Colonization resistance is the phenomenon where established microbial communities prevent the invasion and establishment of new, often pathogenic, species [21, 22, 242523]. This study aims to build upon the findings of Wei et al. [16] by identifying bacterial interaction traits associated with reduced colonization resistance and enhanced transstadial transmission of *Babesia* in ticks. While microbial diversity traits linked to colonization resistance have been extensively studied in vectors like ticks [16] and mosquitoes [17], employing a network-based approach to examine the impact of antibiotics on tick microbiota offers a comprehensive method for evaluating factors affecting microbial community interactions, structure, and functionality. Microbes with co-occurrence patterns are known to be influenced by metabolic interactions and competition for resources [26, 27], offering the potential to capture crucial community characteristics that may not be revealed in analyses based solely on microbial diversity or abundance [27, 28].

Network approach enables the detailed mapping of community interactions [29], potentially revealing how antibiotics disrupt normal microbial relationships

essential for pathogens such as *Babesia*. For example, it can identify how altered interactions of key taxa like *Coxiella* and *Acinetobacter* may compromise the community's ability to resist *Babesia* colonization. By assessing changes in metrics such as modularity and centrality, network analysis provides quantitative evidence of the effects of disturbance on microbial community organization [30]. For instance, increased modularity and altered centrality in antibiotic-treated ticks may indicate a less compartmentalized with strong separation between communities and potentially less resilient microbial network, facilitating *Babesia* establishment and proliferation.

Furthermore, networks allow the evaluation of emerging system properties such as the robustness of microbial communities [30], which allows deciphering how changes impact community structure and function, particularly in response to the loss [29, 31] and addition [31] of specific nodes or bacterial taxa. Ultimately, this approach not only enhances our comprehension of how antibiotics indirectly influence *Babesia* dynamics by altering host microbiota but may also contribute to predictive modelling of disease transmission, offering crucial insights for the effective management of TBDs. Therefore, this study aims to explore the repercussions of antibiotic-induced dysbiosis on microbial interactions within *Haemaphysalis longicornis* ticks. Specifically, it targets the identification of bacterial interaction traits associated with colonization resistance and heightened transstadial transmission of *B. microti*. Employing a network-based approach, the study intends to comprehensively map and analyze the structural, functional, and interactive aspects of tick microbiota under antibiotic exposure. The research holds a scientific merit by elucidating the impact of antibiotics on tick microbiota and subsequent pathogen transmission dynamics. It advances our understanding on the impacts of antibiotics on tick microbiota and subsequent *B. microti* transmission dynamics.

Methods

Original 16S rRNA datasets

In this study, we used available 16S rRNA amplicon sequence datasets generated by Wei et al. [16]. Sequencing was performed on an Illumina MiSeq system and the resultant data has been deposited in the National Center for Biotechnology Information (NCBI)'s GenBank, under Sequence Read Archive (SRA) accession numbers SRP322057 and SRP323180. The raw data was collected as part of a study evaluating the effects of antibiotics on the microbiota of *H. longicornis* ticks and their implications for *B. microti* transmission, comparing the microbiota of nymphal ticks fed on *Babesia microti*-infected mice treated with antibiotics (AT) with the control-treated group (CT).

Analysis of 16S rRNA amplicon sequences

To facilitate a comprehensive exploration of the tick microbiota's composition and function, we retrieved 16S rRNA sequences from the Sequence Read Archive (SRA) repository within the Quantitative Insights Into Microbial Ecology (QIIME2) 2023.7 environment. Briefly, the q-fondue script, following the methodology outlined by Bolyen et al. [32], facilitated the download process. The sequence data (demultiplexed fastq files) underwent denoising, quality trimming, merging, chimera removal, and filtering using DADA2 software [33] implemented within the QIIME2 [32]. Taxonomic assignment to Amplicon Sequence Variants (ASVs) was accomplished using the Classify-Sklearn Naive Bayes method based on the 16S rRNA SILVA database v.138 [34]. The resulting taxonomic table was collapsed at the genus level, and subsequently employed for network analysis and pathway prediction.

Bacterial co-occurrence networks analysis

Co-occurrence networks were constructed for the CT and AT groups using taxonomic information at the genus level to investigate the effect of antibiotic treatment on community assembly. The prevalence of *Coxiella* and *Acinetobacter* within the microbiota in CT and AT groups respectively [16] suggested a possible influence of both taxa on community assembly and stability in response to antibiotic treatment. In addition, global co-occurrence networks were constructed for each condition (CT and AT) after the individual removal of *Coxiella* and *Acinetobacter* to assess their specific impacts. In the graphical visualization of microbial community assemblies, bacterial taxa are represented by nodes and the significant interactions between taxa are represented by edges. Sparse Correlations for Compositional data (SparCC) method [35] implemented in the SpiecEasi R package [36] analysis was used to identify significant positive (weight > 0.75) or negative (weight < -0.75) interactions between taxa, Gephi software 0.10.0 [37] was employed to visualize and analyze network features [i.e. number of nodes and edges, network diameter, modularity, average degree, weighted degree, clustering coefficient and centrality]. Additionally, the Core Association Network (CAN) analysis identified common microbial associations between CT and AT networks, conducted using the Anuran toolbox [38] within the Anaconda Python environment (Anaconda Software Distribution, 2023).

Comparative network analysis

The network comparisons between the same taxa in two different bacterial networks were conducted using the package Network Construction and Comparison for

Microbiome Data (NetCoMi) [39] in R v.4.0.3 (R Core Team, 2023) [40], and performed using RStudio (RStudio Team, 2020) [41]. By comparing networks: (i) between CT and AT groups, (ii) between CT and AT groups after individual removal of *Coxiella* (woC) and *Acinetobacter* (woA), and (iii) within the same CT or AT group in the presence and after the individual removal of both taxa, the study aims to understand how these taxa influence network structure. The Jaccard index was computed to assess dissimilarities in local centrality measures (degree, betweenness centrality, closeness centrality, and eigenvector centrality) between the two networks [i.e., CT vs. AT; CT vs. CT (woC); CT (woC) vs. AT (woC)], providing insights into the impact of antibiotic treatment and taxa presence and absence on network structure. This index evaluates the similarity between sets of 'most central nodes' in networks, defined as nodes with centrality values above the empirical 75% quartile. It ranges from 0 (totally different) to 1 (unique). The associated *p*-values, $P(J \leq j)$ and $P(J \geq j)$, indicate the probability that the observed Jaccard index value is 'less than or equal to' or 'higher than or equal' to' the Jaccard value expected at random, considering the total number of taxa in both sets [42]. The ARI was calculated to test the dissimilarity of clustering in the networks. ARI values range from -1 to 1. Negative and positive ARI values mean lower and higher than random clustering, respectively. An ARI value of 1 corresponds to identical clustering, and 0 to dissimilar clustering. The *p*-value test if the calculated value is significantly different from zero [39].

Local connectivity of *Acinetobacter* and *Coxiella* in the microbial community

The effect of antibiotic treatment on specific taxa was analyzed by determining the direct associations of *Acinetobacter* and *Coxiella* with the rest of the bacterial microbiota in the CT and AT groups. This analysis aimed to understand how these taxa influenced the overall microbial community structure. Sub-networks representing the positive and negative associations of local connectivity were constructed in Gephi 0.10.0 [37], with connections between microbes quantified using SparCC ($SparCC > 0.75$ or < -0.75) as implemented in the SpiecEasi R package [36], enabling the identification of key microbial associations influenced by antibiotic treatment.

Centrality measures and module dynamics in networks of CT and AT microbiota

To understand the networks structure of the CT and AT groups, the centrality measures distribution among different taxa, including *Coxiella* and *Acinetobacter*, were analyzed. The function of each taxon within the network was assessed using measures of within-module (Zi) and among-module (Pi) connectivity [43]. The measures allowed the taxa to be categorized into four different roles according to their connectivity: (i) network hubs: taxa that serve as central connectors both within their module and across the entire network, with high connectivity ($Zi > 2.5$ and $Pi > 0.62$), (ii) module hubs: highly connected taxa within their own module but not significantly connected to other modules ($Zi > 2.5$ and $Pi \leq 0.62$), (iii) connectors: taxa that primarily link different modules together, indicating their role in connecting disparate parts of the network ($Zi \leq 2.5$ and $Pi > 0.62$), and (iv) peripheral taxa: taxa with limited connections within the module and minimal interactions with other modules ($Zi \leq 2.5$ and $Pi \leq 0.62$). The Zi and Pi values were calculated using the "code-zi-pi-plot" package [44, 45] in R (R Core Team, 2023) [40], considering only positive interactions. Visualization was done using GraphPad Prism version 8.0.1 (GraphPad Software, San Diego, California, USA), enabling the analysis of taxon positions within the networks. This analysis helps identify major key players influencing community assembly in response to antibiotic treatment.

Identification of keystone taxa

To pinpoint microbial taxa that play crucial roles in maintaining the stability and function of the tick microbiota, keystone taxa were identified based on three criteria as described by Mateos-Hernandez et al. [46]: (i) ubiquitousness (microbial taxa present across all the samples of an experimental group), (ii) eigenvector centrality higher than 0.75, and (iii) abundance higher than the mean clr value (i.e., higher than that of the mean relative abundance of all taxa in an experimental group).

Network robustness analysis using node removal and addition

The stability of the CT and AT networks was evaluated and compared to determine if antibiotic treatment impacts the stability and resilience of the tick microbiota network in response to node disturbances. The robustness of the networks was compared under two types of disturbances: node removal and addition. The comparisons were made between: (i) CT and AT groups, (ii) CT and AT groups after individual removal of *Coxiella* and *Acinetobacter*, and (iii) within the same CT or AT group in the presence and after the individual removal of each taxon. To evaluate network resistance to node removal, an attack tolerance test was conducted using Network Strengths and Weaknesses Analysis (NetSwan) [47] in R v.4.0.3 (R Core Team, 2023) [40], performed using the RStudio (RStudio Team, 2020) [41]. The networks underwent both random and directed attacks. For directed node removal, three scenarios were employed: (i) a

directed attack removing nodes in decreasing order of their betweenness centrality (BNC) value, (ii) a cascading attack recalculating BNC values after each node removal, and (iii) a degree centrality removal prioritizing nodes with the highest degree centrality values.

Conversely, a node addition analysis was performed following the approach outlined by Freitas et al. [48] in R v.4.3.1 (R Core Team, 2023), and performed using the RStudio (RStudio Team, 2020) [41]. In this analysis, new nodes were randomly connected to the existing network, and resultant changes were quantified by evaluating the size of the Largest Connected Component (LCC) and the Average Path Length (APL). To enhance the precision of the network's robustness assessment, multiple simulations were conducted with varying sets of nodes, introducing 500, 700, and 1000 nodes. The outcomes were graphically represented using GraphPad Prism 9.0.2 (GraphPad Software Inc., San Diego, CA, USA). For all comparisons made between the control (CT, CT (woC) and CT (woA)) and antibiotic-treated (AT, AT (woC) and AT (woA)) groups, a delta value was calculated. For node removal analysis, it was the difference in the fraction of nodes needed to achieve a connectivity loss of 0.80. For the addition of nodes, delta values for LCC size and APL were calculated by subtracting values in the CT network from those in the AT network after adding 100 and 1000 nodes.

Functional profile prediction

A step-forward analysis was performed to predict microbial functional traits, specifically enzymatic pathways, utilizing PICRUSt2 (Phylogenetic Investigation of Communities by Reconstruction of Unobserved States) standalone version [49]. Gene catalogues, including Kyoto Encyclopedia of Genes and Genomes (KEGG), Orthologs (KO), Enzyme Classification numbers (EC), and Cluster of Orthologous Genes (COGs) [50], along with the MetaCyc database [51], were employed to annotate major pathway categories and facilitate mapping. Following the output table, the taxa's contribution to predicted metabolic pathways was investigated. To ensure robust statistical analysis, various methods were employed. Initially, alpha diversity was assessed using observed features [52] and Pielou's evenness metrics [53] via the q2-diversity method in QIIME2 plugin. Subsequently, differences in pathway frequency were evaluated using the DESeq2 package [54] in R v.4.0.3 (R Core Team, 2023) [40], enabling the identification of statistically significant alterations in pathway abundance between the CT and AT groups. This analysis resulted in a Volcano plot with Benjamini correlation, providing a visual representation of the significance and magnitude of pathway abundance changes. Analyses were performed using the RStudio Integrated Development Environment (IDE) v.2023.03.0-daily+82.pro2 (RStudio Team, 2020) [41].

Results

Changes in microbial community assembly and node centrality in response to antibiotic treatment

The potential impact of antibiotics on the assembly of microbial communities in ticks' microbiota and the infection of *Babesia* was investigated, specifically examining changes beyond bacterial composition, richness, and relative abundance. To explore this, microbial co-occurrence patterns through co-occurrence networks were analyzed. It was observed that AT exhibited a greater number of connected nodes compared to CT, showing topological variations between both groups (Table 1). In contrast, CT displayed the highest number of correlations compared to AT (Fig. 1 A-B, Table 1). However, a similar balance between positive and negative correlations was observed in both groups (Table 1), suggesting that antibiotic treatment reduces the level of interaction within the community but does not change its nature. Additionally, CT displayed lower modularity and diameter values than AT (Table 1). The core association network (CAN) revealed

Table 1 Topological features of taxonomic co-occurrence networks

Topological features	CT[a]	AT[b]	CT (woC)	AT (woC)	CT (woA)	AT (woA)
Connected nodes	106	115	105	114	103	114
Edges	2245	1095	2206	1079	2202	1104
Positives	1305 (58.1%)	653 (59.6%)	1274 (57.8%)	641 (59.4%)	1277 (58%)	435 (39.4%)
Negatives	940 (41.9%)	442 (40.4%)	932 (42.2%)	438 (40.6%)	925 (42%)	669 (60.6%)
Modularity	1.54	1.64	1.56	1.66	1.59	1.61
Network diameter	5	7	5	7	5	7
Average degree	42.36	19.04	42.02	18.93	47.75	19.37
Weighted degree	7.059	3.583	6.69	3.47	7.02	3.93
Clustering coefficient	0.809	0.753	0.82	0.76	0.82	0.77

[a] Control group (CT networks at threshold of 0.75). [b]Antibiotics group (AT, networks at threshold of 0.75)

71 core associated nodes between CT and AT networks (Fig. 1C) demonstrating variability in community configuration in these two conditions. NetCoMi was used to test dissimilarities between local network centrality measures of the CT and AT networks, Jaccard index was calculated for degree, betweenness centrality, closeness centrality and eigenvector centrality (Jacc = 0, lowest similarity and Jacc = 1, highest similarity). All these measures between the two networks were found to be lower than expected by random (P (≤ Jacc) < 0.05, Table 2).

The most abundant genera in the CT adults were *Ammoniphilus* and *Coxiella*. However, the gut microbiota in AT adults was dominated by *Acinetobacter* [16]. To understand the role of *Coxiella* and *Acinetobacter* in the community assembly, the local connectivity in the CT and AT groups was visually inspected. Both networks displayed two principal modules with negative and positive co-occurring interactions between their nodes. In the CT group's microbial community of infected ticks with *Babesia*, *Coxiella* occupied a central position, displaying numerous interactions with other genera (Fig. 1D, Supplementary Table S1). However, visual inspection of the networks showed that the treatment caused a shift in the bacterial community assembly patterns with a notable reduction in *Coxiella*'s co-occurrence network with other taxa (Fig. 1E, Supplementary Table S1). Although the local connectivity sub-networks between CT and AT groups were unique in their connections, *Coxiella* maintained common direct association with four taxa in both networks (Fig. 1F). Similarly, *Acinetobacter* in CT showed high centrality and extensive connections with various taxa (Fig. 1G, Supplementary Table S1). Antibiotics disrupted *Acinetobacter*'s interactions, reducing its connectivity and affecting the microbial community co-occurrence network resulting in a loss of a few connected nodes (Fig. 1H, Supplementary Table S1). However, *Acinetobacter* maintained a common direct association with eight taxa in both groups (Fig. 1I). Markedly, *Coxiella* and *Acinetobacter* presented a direct association of co-exclusion, which was maintained in the AT group (Fig. D-I, Supplementary Table S1).

When analyzing the distribution of connections (Zi and Pi connectivity), a similar pattern was observed in both CT (Fig. 1J) and AT (Fig. 1K) networks. All taxa, including *Coxiella* and *Acinetobacter*, were classified as peripheral, indicating that they do not function as central hubs within their respective networks. Despite the absence of central nodes within CT and AT networks, eight taxa met the criteria to be considered keystone taxa for the CT and six for the AT group microbiota (Table 3). In general, the topological variations, the changed clustering patterns of *Coxiella* and *Acinetobacter* and the absence of other central hubs demonstrate notable differences in community assembly between both conditions and a considerable susceptibility to antibiotic treatment. This behavior suggests a possible influence of both taxa on community assembly as support for the destabilizing effect that antimicrobial treatment can cause.

Table 2 Jaccard index for comparison between CT and AT network

Local centrality measures	CT *vs.* AT		
	Jaccard	P(≤ Jacc)	P(≥ Jacc)
Degree Centrality	0.098	0.000096 ***	0.999981
Betweenness Centrality	0.071	0.000004 ***	0.999999
Closeness Centrality	0.111	0.000163 ***	0.999962
Eigenvector Centrality	0.200	0.028440 *	0.987292
Hub taxa	0.200	0.028440 *	0.987292

Jaccard index for co-occurrence networks with the threshold of 0.75, *$p < 0.05$, ***$p < 0.0002$

Influence of *Coxiella* and *Acinetobacter* on the assembly and hierarchy of the microbiota in response to antibiotic treatment

To investigate the impact of *Coxiella* and *Acinetobacter* on community assembly in response to antibiotic treatment, the topology of the network was analyzed after individual removal of both taxa (woC and woA), comparing the CT and AT groups (Table 1). Removal of *Coxiella* resulted in a loss of interactions in both CT (woC) and AT (woC) networks (Fig. 2 A-B, Table 1) compared to conditions with the taxon present (Table 1), suggesting potential stability conferred by the bacteria in its endosymbiont condition. Similar to those observed in the

(See figure on next page.)

Fig. 1 Antibiotic treatment effects on microbiota diversity and community assembly in *Babesia*-infected ticks. Global co-occurrence networks of (**A**) CT and (**B**) AT networks. **C** Core Association Network between CT/AT networks. *Coxiella*'s local connectivity in (**D**) CT and (**E**) AT networks. **F** Direction of associations of common direct neighbor to *Coxiella* between CT and AT groups. *Acinetobacter*'s local connectivity in (**G**) CT and (**H**) AT networks. **I** Direction of associations of common direct neighbor to *Acinetobacter* between CT and AT groups. Within-module and among-module connectivity, Zi-Pi plot of the individual genera from (**J**) CT and (**K**) AT groups. Only nodes with at least one significant correlation are represented. Node colors are based on modularity class metric and equal color means modules of co-occurring taxa. The size of the nodes is proportional to the eigenvector centrality of each taxon. The colors in the edges represent strong positive (green) or negative (red) correlations (SparCC > 0.75 or < −0.75)

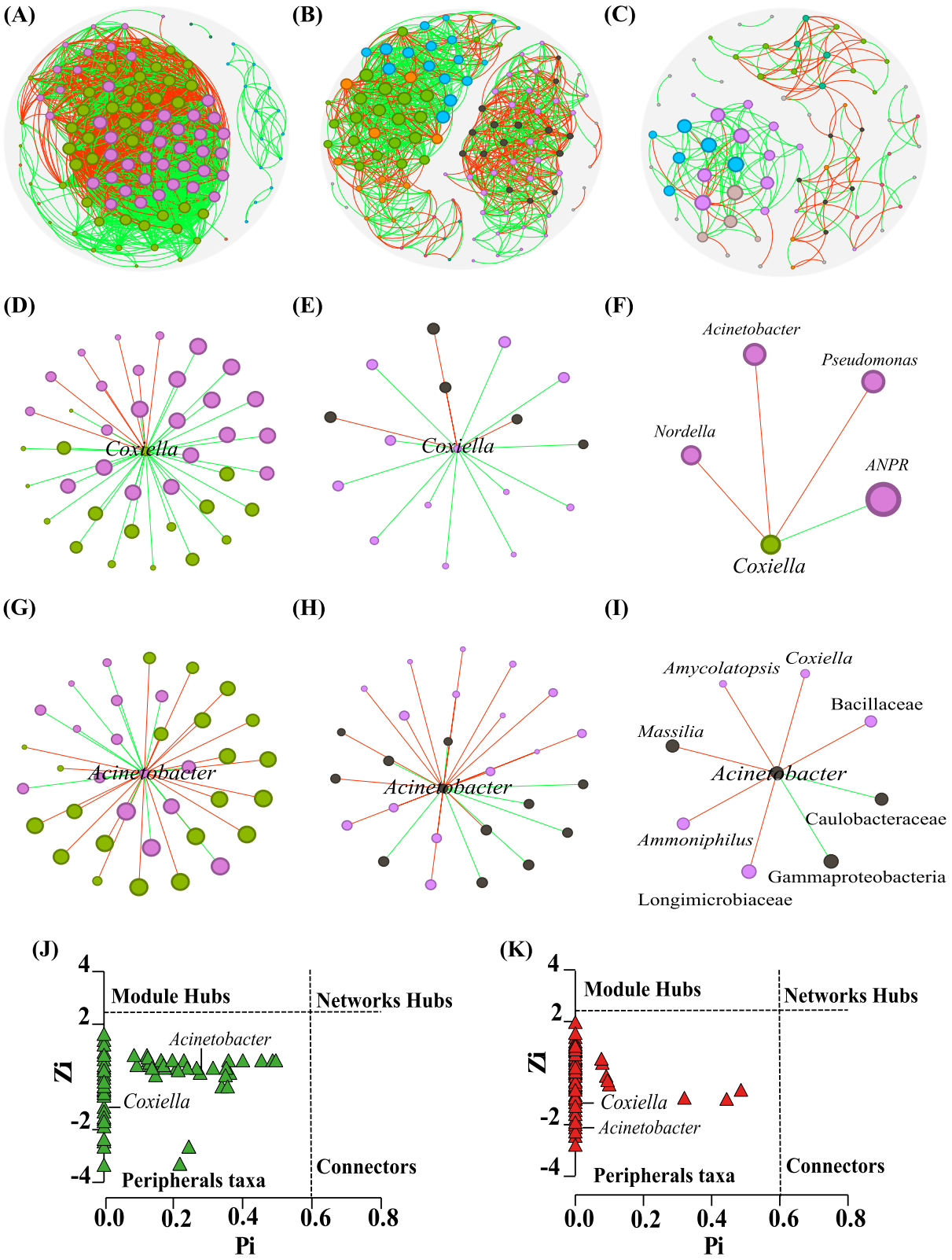

Fig. 1 (See legend on previous page.)

Table 3 Keystone taxa of the bacterial communities of CT and AT groups

Condition	Keystone taxa by condition
CT	*Ammoniphilus* *Noviherbaspirillum* Microtrichales *Brevundimonas* *Amycolatopsis* *Nocardia* Symbiobacteraceae Longimicrobiaceae
AT	*Methyloceanibacter* *Lysobacter* Comamonadaceae *Methylonatrum* *Sediminibacterium* Xanthobacteraceae

presence of *Coxiella*, there was a balance between positive and negative interactions in the CT (woC) and AT (woC) networks, with cooperation being slightly greater (Fig. 2 A-B, Table 1). Moreover, after removing *Acinetobacter*, a decrease in the number of interactions was observed in both CT (woA) and AT (woA) (Fig. 2 C-D, Table 1) compared to conditions with the taxon present. However, a disproportion between positive and negative associations was evident in AT (woA) compared to CT (woA) (Fig. 2 C-D, Table 1), indicating increased competition post-taxa removal. Furthermore, the decrease in interactions of cooperation and co-exclusion (Table 1), upon comparing networks of the same condition after individual bacteria removal suggests a reconfiguration of the remaining taxa.

The impact of individual removal of *Coxiella* (woC) and *Acinetobacter* (woA) on the interaction patterns between CT and AT networks (Table 4) were compared,

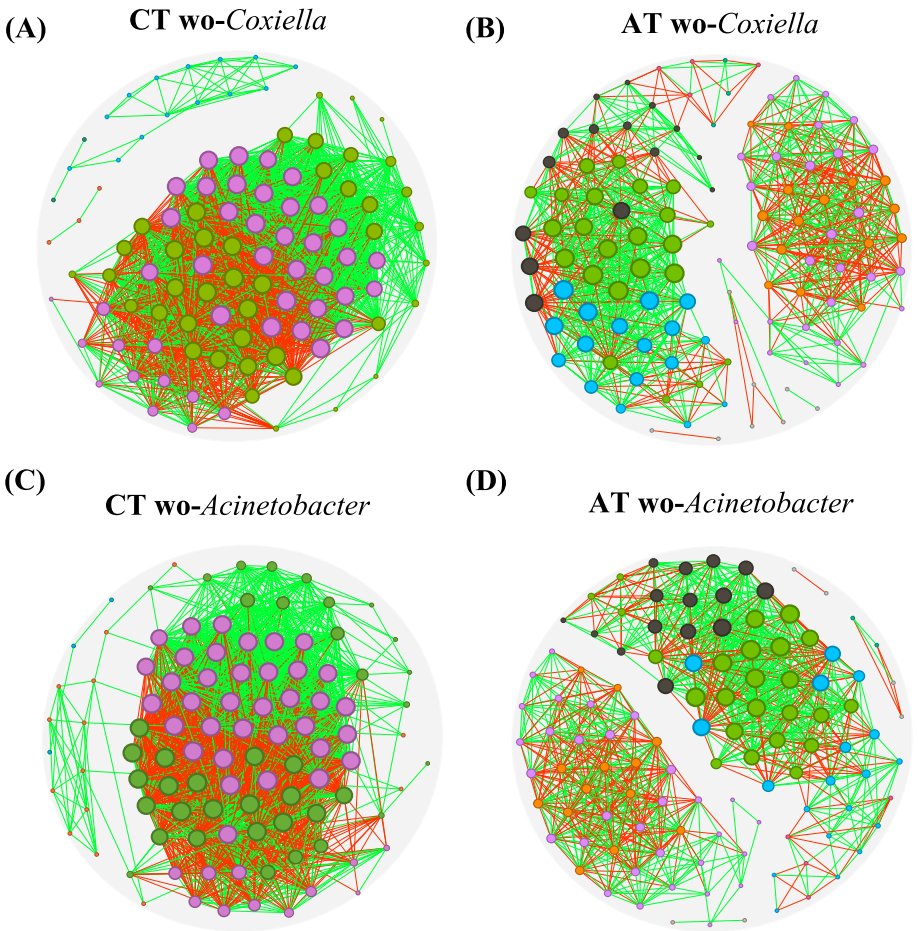

Fig. 2 Comparative analysis of microbial co-occurrence networks in CT and AT groups: Impact of *Coxiella* and *Acinetobacter* removal. Global co-occurrence networks after *Coxiella*'s removal of (**C**) CT(woC) and (**D**) AT(woC). Global co-occurrence networks after *Acinetobacter*'s removal of (**E**) CT(woA) and (**F**) AT(woA). The colors in the edges represent positive (green) or negative (red) correlations. In global networks, the node colors are based on modularity class metric and equal color means modules of co-occurring taxa. The size of the nodes is proportional to the eigenvector centrality of each taxon

Table 4 Jaccard index for comparison between CT and AT groups after *Coxiella* and *Acinetobacter*'s removal

Local centrality measures	CT (woC) *vs.* AT (woC)			CT (woA) *vs.* AT (woA)		
	Jaccard	P(≤ Jacc)	P(≥ Jacc)	Jaccard	P(≤ Jacc)	P(≥ Jacc)
Degree Centrality	0.135	0.001021 **	0.999708	0.059	0.000003 ***	1.000000
Betweenness Centrality	0.111	0.000163 ***	0.999962	0.111	0.000163 ***	0.999962
Closeness Centrality	0.154	0.003070 **	0.998979	0.200	0.028440 *	0.987292
Eigenvector Centrality	0.176	0.010149 *	0.996063	0.154	0.003070 **	0.998979
Hub taxa	0.176	0.010149 *	0.996063	0.154	0.003070 **	0.998979

Jaccard index for co-occurrence networks with the threshold of 0.75, *$p < 0.05$, **$p < 0.005$, ***$p < 0.0002$

Table 5 Network clustering comparisons

Conditions	Network comparison	Adjusted Rand index (ARI)	*p*-value
Without *Coxiella* (woC)	**CT (woC) *vs.* AT (woC)**	-0.002	0.87
Without *Acinetobacter* (woA)	**CT (woA) *vs.* AT (woA)**	-0.011	0.36
CT-*Coxiella*	**CT *vs.* CT (woC)**	0.71	0
AT-*Coxiella*	**AT *vs.* AT (woC)**	0.98	0
CT-*Acinetobacter*	**CT *vs.* CT (woA)**	0.93	0
AT- *Acinetobacter*	**AT *vs.* AT (woA)**	0.96	0

as well as within the same condition before and after *in-silico* manipulation of the taxa (Supplementary Table S2 and S3). Jaccard index values were lower than expected by random (P (≤ Jacc) < 0.05) in woC (CT *vs.* AT) and woA (CT *vs.* AT) comparison, respectively (Table 4). Moreover, the centrality measures were higher than expected by random (P (≥ Jacc) < 0.05) in CT *vs.* CT (woC) (Supplementary Table S2) and CT *vs.* CT (woA) (Supplementary Table S3) comparison, respectively. Jaccard index values of the AT *vs.* AT (woC) and AT *vs.* AT (woA) comparisons, were higher than expected by random (P (≥ Jacc) < 0.05) except for betweenness centrality and closeness centrality which had a random distribution. Comparing node clustering for woC (CT vs. AT) and woA (CT vs. AT) revealed low ARI values, indicating the antibiotic treatment strongly influences microbial community clustering patterns (Table 5). In contrast, ARI values were close to 1 within the same condition (CT and AT) after individual taxon removal (Table 5). High ARI values indicated strong similarities and suggested that despite the topological variations (Table 1) the impact of *in-silico* manipulation of *Coxiella* and *Acinetobacter* on clustering patterns under the same conditions is moderated.

Changes in network robustness in response to antibiotic treatment

The robustness of the CT and AT co-occurrence networks was compared to determine if the effect of antibiotic treatment compromises stability against node removal and addition. Assessment of connectivity loss showed that directed attacks (degree, cascading, and betweenness methods) (Fig. 3A-B and Supplementary Fig. S1A) had more significant impacts on both CT and AT networks compared to the random method (Supplementary Fig. S1B, Supplementary Table S4). During node removal, delta values were calculated by subtracting the fraction of nodes necessary to achieve a connectivity loss of 0.8 of CT minus AT network. Degree-directed node removal yielded a negative delta value, indicating AT's greater robustness compared to CT (Fig. 3A, Supplementary Table S4). Conversely, cascading and betweenness node removal showed positive values, suggesting antibiotic treatment reduces network stability against both types of directed attacks (Fig. 3B, Supplementary Fig. S1A, Supplementary Table S4). The delta value equal to 0 confirms that, regardless of the possible community-destabilizing effect of antibiotic treatment, the robustness of the CT and AT networks is not affected by random attacks (Supplementary Fig. S1B, Supplementary Table S4). Comparing robustness against node removal between CT and AT networks after individual *Coxiella* (Fig. 3C-D, Supplementary Fig. S1C-D) and *Acinetobacter* (Fig. 3E-F, Supplementary Fig. S1E-F) removal showed that only in the absence of *Coxiella* and after directed attack in degree and betweenness, the AT network was more robust than the CT network (Fig. 3C and Supplementary Fig. S1C). Additionally, positive delta values in the absence of *Acinetobacter* and after directed attack in degree and cascading (Fig. 3E-F) highlight the susceptibility of the AT group to external perturbations and suggest a possible stabilizing potential exerted by the taxon when present (Supplementary Table S4).

For node addition, 1000 nodes were added, and two key network properties were quantified: LCC (Fig. 3G, Supplementary Table S5) and APL (Fig. 3H, Supplementary

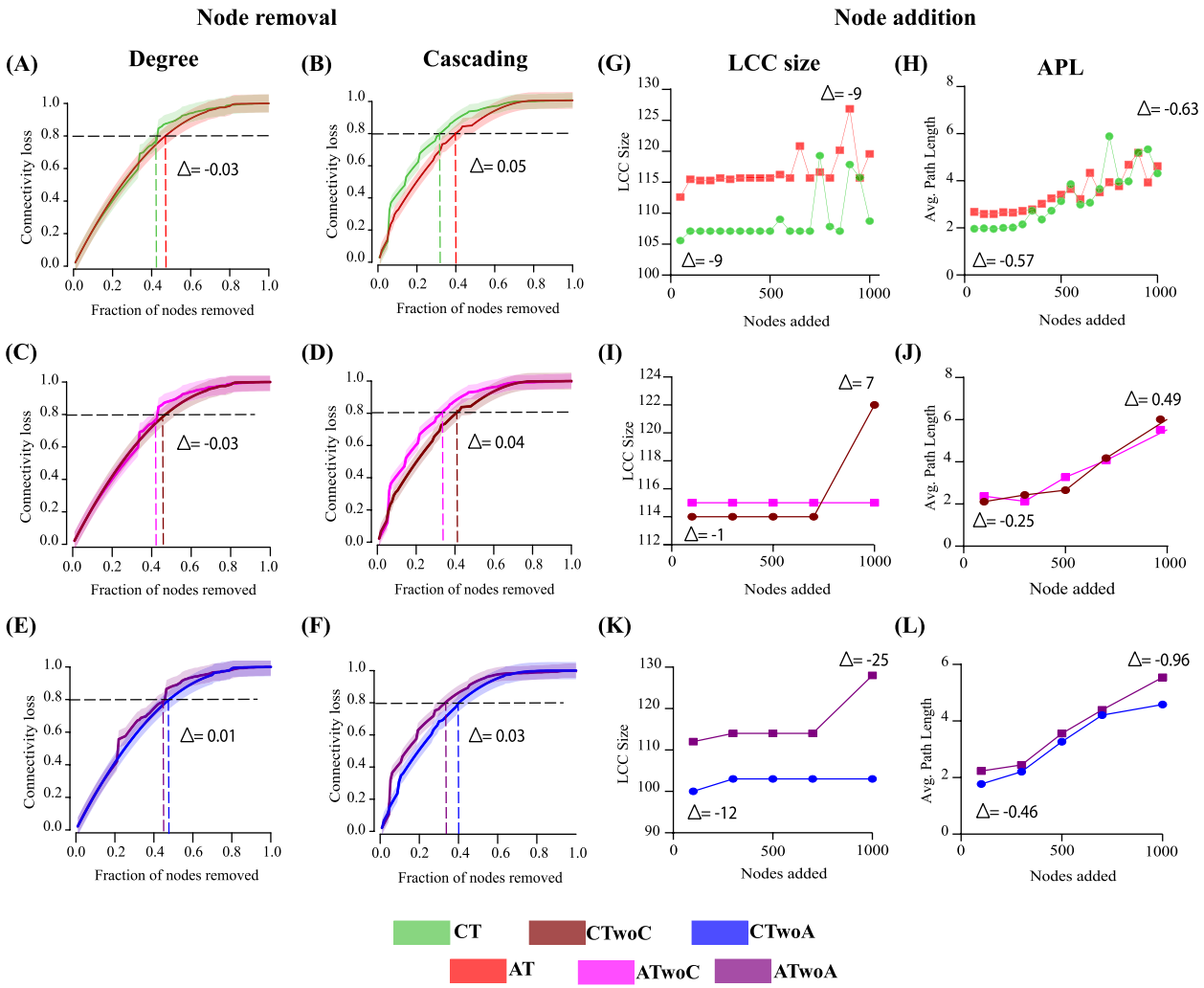

Fig. 3 Robustness comparison after removal and addition of nodes between the CT and AT groups. Connectivity loss measured after directed (degree and cascading) attack in CT and AT networks: (**A**) CT/AT (degree), and (**B**) CT/AT (cascading), Connectivity loss measured against directed (degree and cascading) attack between the CT and AT networks after *Coxiella*' removal: (**C**) CT(woC)/AT(woC) (degree), and (**D**) CT(woC)/AT(woC) (cascading). Connectivity loss measured against directed (degree and cascading) attack between the CT and AT networks after *Acinetobacter*'s removal: (**E**) CT(woA)/AT(woA) (degree), and (**F**) CT(woA)/AT(woA) (cascading). Robustness comparison between CT and AT networks after the addition of nodes. The largest connected component (LCC) and average path length (APL) values are represented and compared between CT and AT networks: (**G**) CT/AT (LCC), and (**H**) CT/AT (APL). Robustness comparison between CT and AT networks after *Coxiella*'s removal: (**I**) CT(woC)/AT(woC) (LCC), and (**J**) CT(woC)/AT(woC) (APL). Robustness comparison between CT and AT networks after *Acinetobacter*'s removal: (**K**) CT(woA)/AT(woA) (LCC), and (**L**) CT(woA)/ AT(woA) (APL)

Table S5). Applying the nodes addition strategy increased the LCC for the AT group compared to the CT group (Fig. 3G, Supplementary Table S5). Specifically, The AT group's average robustness increased at the 750th node addition, followed by a similar rise in the CT group at the 800th node addition. Both groups showed a rapid increase in robustness by the 900th node added. Regarding the APL test, initially, the AT group exhibited slightly higher values than the CT group until the addition of the 800th node, after which the CT network rapidly increased (Fig. 3H, Supplementary Table S5). Ultimately, APL values for both groups converged to approximately equal values upon the addition of 1000th node. However, the observed overlap and increase in APL values in both CT and AT networks suggest that the addition of nodes causes a loss of functional connectivity within the networks independently of the effect of antibiotic treatment (Fig. 3H, Supplementary Table S5). The higher LCC and APL values of AT compared to CT were highlighted by negative delta values after adding the 100th and 1000th nodes (Fig. 3G-H, Supplementary Table S5). This persisted after *Coxiella* (Fig. 3I-J) and *Acinetobacter*

(Fig. 3K-L) removal, with higher LCC and APL values in AT networks Fig. 3I-L, Supplementary Table S5), except for LCC values after adding the 1000th nodes in *Coxiella*-removed networks, showing a positive delta value (Fig. 3I, Supplementary Table S5).

Influence of the removal of *Coxiella* and *Acinetobacter* on network robustness within the CT and AT groups

To demonstrate the direct influence of both bacteria within the same condition (CT or AT) after node removal, the robustness of the networks was analyzed and compared after individual removal of *Coxiella* (woC) (Fig. 4A-D, Supplementary Fig. S2A-D) and *Acinetobacter* (woA) (Fig. 4E-H, Supplementary Fig. S2E-H). The removal of *Coxiella* did not modify the robustness of the networks within the same condition against directed (Fig. 4A-D) and random attacks (Supplementary Fig. S2A-D). In contrast, the removal of *Acinetobacter* conferred robustness and stability to the AT (woA) network during a connectivity loss of 0.8 after the directed attack in degree (Fig. 4F) and, in addition, to CT (woA) network in betweenness (Fig. 4G). This behavior highlights the important role of *Acinetobacter* within the community conditioned by its high abundance and possible potential for antibiotic resistance.

During the addition of nodes, the LCC values was higher in the CT network following *Coxiella* removal (Fig. 5A). In contrast, an overlap was observed between the AT and AT (woC) networks (Fig. 5B), suggesting that the absence of the taxon did not influence the response to the addition of nodes. On the other hand, the presence of *Acinetobacter* conferred stability in both CT and AT conditions (Fig. 5C-D). The robustness conferred by *Acinetobacter* may be due to its potential for resistance to antibiotic treatment and therefore its possible action in maintaining stability. Interestingly, only the LCC value measured in the AT network after the addition of 1000 nodes demonstrated greater robustness in the absence of the taxon (Fig. 5D). The overlap and increase in APL values within the same condition for the CT and AT groups in the presence and after the individual removal of each taxon continue to suggest loss of functional connectivity and increase in competition within the network with the addition of nodes (Fig. 5E-H).

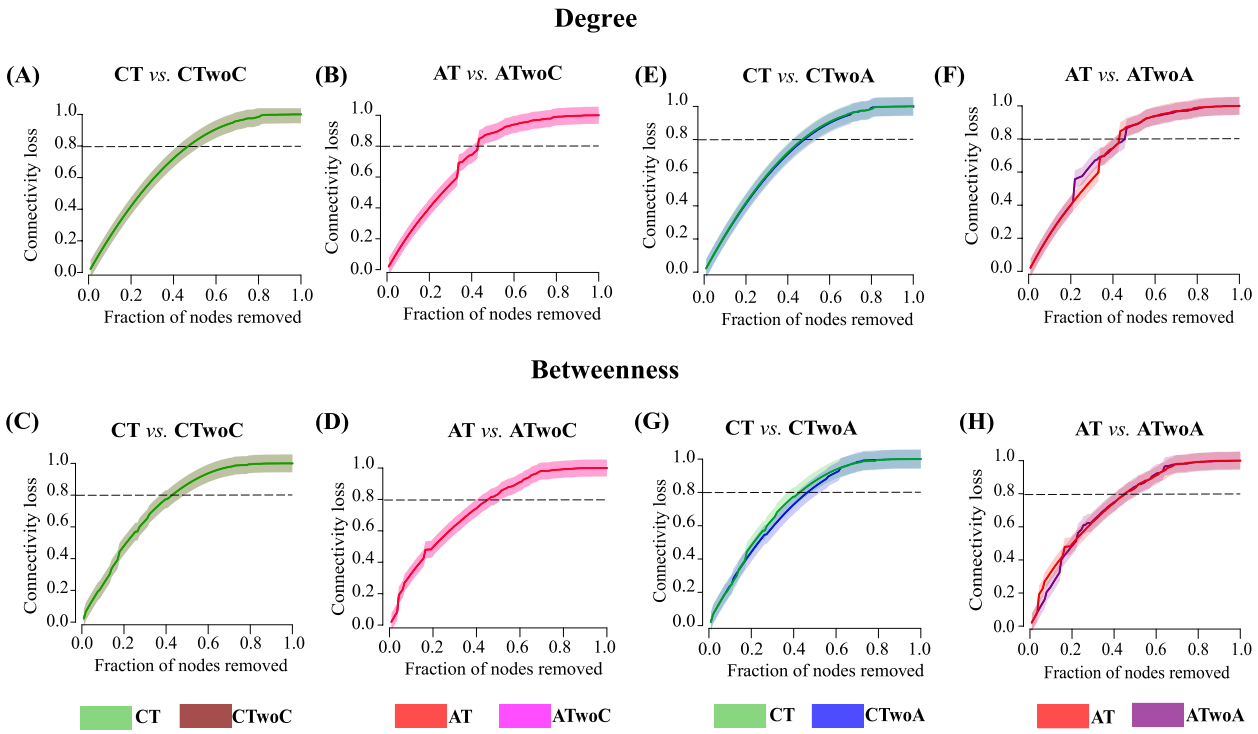

Fig. 4 Robustness comparison after node removal within groups (CT and AT). Connectivity loss measured after directed attack (degree and betweenness) in *Coxiella*'s presence (wC) and removal (woC): (**A**) CT (wC *vs.* woC) and (**B**) AT (wC *vs.* woC) in degree, (**C**) CT (wC *vs.* woC), and (**D**) AT (wC *vs.* woC) in betweenness. Connectivity loss measured after directed attack (degree and betweenness) in *Acinetobacter*'s presence (wA) and removal (woA) between the same group: (**E**) CT (wA *vs.* woA), and (**F**) AT (wA *vs.* woA) in degree, (**G**) CT (wA *vs.* woA), and (**H**) AT (wA *vs.* woA) in betweenness

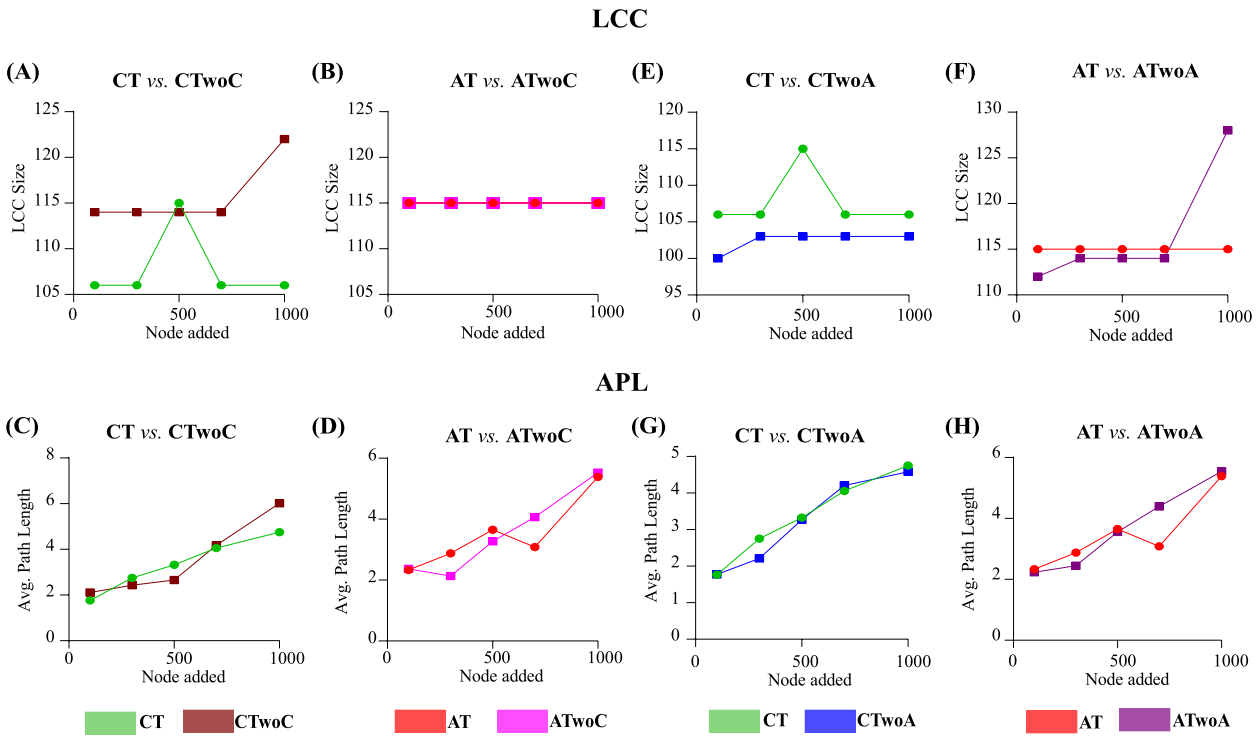

Fig. 5 Robustness comparison against addition of nodes after taxa's removal between the same groups (CT and AT). LCC values are represented and compared in *Coxiella*'s presence and removal between the same groups: (**A**) CT (wC *vs.* woC), and (**B**) AT (wC *vs.* woC). LCC values are represented and compared in *Acinetobacter*'s presence and removal between the same groups: (**C**) CT (wA *vs.* woA), and (**D**) AT (wA *vs.* woA). APL values are represented and compared in *Coxiella*'s presence and removal between the same groups: (**E**) CT (wC *vs.* woC), and (**F**) AT (wC *vs.* woC). APL values are represented and compared in *Acinetobacter*'s presence and removal between the same groups: (**G**) CT (wA *vs.* woA), and (**H**) AT (wA *vs.* woA)

Changes in predicted functional profiles in response to antibiotic treatment

The alterations in microbial community composition and structure were assessed to determine whether they affected the inferred functional profile of tick microbiota. A thorough analysis was conducted, comparing the composition, diversity, and relative abundance of metabolic pathways in the microbiota of *H. longicornis* ticks from both the AT and CT groups. The investigation revealed a greater richness in functional profiles within the AT group compared to the CT group. Specifically, diversity metrics such as observed features (Fig. 6A) and Pielou's evenness index (Fig. 6B) were higher for the AT group compared to the CT group. Differences were also observed in the relative abundance of pathways between the functional profiles of AT and CT groups (Fig. 6C, Supplementary Table S6). Analysis revealed both unique and shared predicted metabolic pathways within the microbiota of both groups. Specifically, five pathways were identified as unique to the CT tick microbiota, while the AT tick microbiota exhibited eleven unique pathways within which the 2-heptyl-3-hydroxy-4(1H)-quinolone biosynthesis pathway is found (Fig. 6D, Supplementary Table S7 and 8). Furthermore, both microbiota shared 398 pathways (Fig. 6D, Supplementary Table S7 and 8), predominantly associated with biosynthesis, as documented on MetaCyc database [51].

Discussion

Our findings provide support for the hypothesis that antibiotic treatment (AT) disrupts the microbial community assembly and network interactions within *H. longicornis* ticks. This disruption affects key taxa such as *Coxiella* and *Acinetobacter*, and complement those of Wei et al. [16] in understanding how antibiotics disrupt colonization resistance within tick microbiota, thereby facilitating the transstadial transmission of *B. microti*. Colonization resistance is a critical ecological function provided by the native microbiota as it prevents the establishment and proliferation of pathogens within the host [55]. This resistance is mediated by several mechanisms, including competition for resources [26, 27] and modulation of the host's immune response [56, 57]. The network-based traits associated with AT and their influence on reduced colonization resistance and enhanced *Babesia* transstadial transmission can be summarized: 1) the AT group

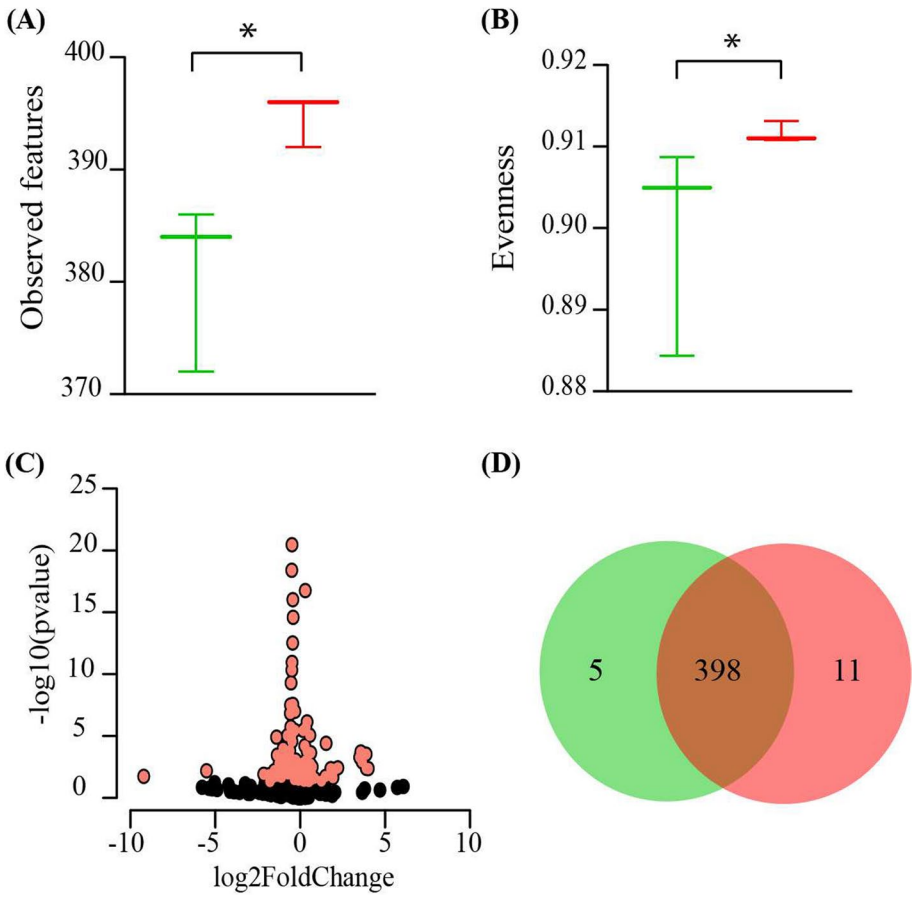

Fig. 6 Predicted functional profile analysis. Comparative analysis of predicted functional profiles between CT (green) and AT groups (red). **A** Observed features, and (**B**) Pielou's evenness index were employed to assess pathway alpha diversity. **C** Differential abundance of predicted metabolic pathways. Volcano plot showing the differential abundance of pathways in CT and AT microbiota. The pathways with significant differences (Wald test, $p < 0.05$) between the groups are represented by pink dots. **D** Venn diagram illustrates shared and unique predicted bacterial pathways between the CT and AT microbiota

had more connected nodes but less interactive microbial community compared to the CT group. 2) Despite having more connections, the AT group had fewer correlations and greater modularity compared to the CT group. 3) There were significant differences in network centrality measures between AT and CT groups and in the connectivity and network roles of key taxa such as *Coxiella* and *Acinetobacter*. 4) The robustness tests (i.e., node removal strategies) demonstrated that the AT networks were less stable against specific attacks compared to CT networks. And 5) The AT group displayed a greater richness in functional profiles.

Enhanced network connectivity and modularity in AT microbiota

Antibiotic treatment modifies the community assembly as a consequence of the reduction of microorganisms due to its bacteriostatic or bactericidal effect [58, 59]. Consequently, interactions such as co-occurrence (positive correlation) or co-exclusion (negative correlation) may change [60, 61]. We found topological variations indicating distinct community assembly between the CT and AT groups, with a decrease in the number of interactions between community members. However, no considerable changes were evident in the nature of the interactions, with a balance between cooperation and co-exclusion existing in both groups. This change in topology may reflect a shift towards a microbial community where fewer dominant interactions exist, potentially reducing competitive exclusion and colonization resistance. The interactions established between microorganisms within communities can alter the susceptibility of their members to antibiotic treatment [57]. The nature and number of interactions established can determine whether the resistance of a microbial species to a certain antibiotic confers a protective effect [57, 62].

Altered centrality measures

Analyzing antibiotic effects on node centrality and network strength in *Babesia*-infected ticks' co-occurrence networks revealed significant insights into microbial interaction dynamics under perturbations. Specifically, differences in local network centrality measures (degree, betweenness centrality, closeness centrality, and eigenvector centrality) between CT and AT groups highlights distinct microbial network patterns. Interestingly, the AT group showed greater adaptability to disruptions with additional nodes, while both groups exhibit similar overall robustness. Furthermore, taxa such as *Coxiella* and *Acinetobacter* showed disrupted connectivity in the AT group. *Coxiella* exhibited reduced interactions, whereas *Acinetobacter* experiences a loss of connected nodes, underscoring their critical roles in maintaining microbial network stability. This provides insights by demonstrating differences in network centrality measures and the roles of key taxa like *Coxiella* and *Acinetobacter* between both groups which deepen our understanding of how antibiotic treatment impacts tick microbiota dynamics.

Impact of key taxa including *Coxiella* and *Acinetobacter*

In their initial study, Wei et al. [16] observed that antibiotic treatment led to a significant alteration in the diversity and abundance of the tick gut microbiota. They noted shifts towards genera like *Acinetobacter*, known to thrive under antibiotic pressure [16], and a decreased in *Coxiella*, which typically acts as an endosymbiont in ticks [63], providing protection against tick-borne pathogens (TBPs) [55, 64]. This alteration suggests a disruption of the balanced microbial ecosystem that typically supports colonization resistance to *Babesia* infection. Our study further demonstrated that these shifts are not just alterations in abundance but also critical changes in the connectivity and network roles of key taxa such as *Coxiella* and *Acinetobacter*. The reduced interaction within the microbial community and the loss of connected nodes indicates a weakened network structure, reducing the microbiota's ability to collectively resist new colonization by pathogens, in this case, *Babesia* species. Symbiont-mediated protection, predicted through ecological modelling, is increasingly observed in natural insect populations, serving as a potent mechanism to maintain symbiont prevalence [55]. Ticks harbor various nutritional symbionts, including *Coxiella*-like endosymbionts (CLE) [65], *Francisella*-like endosymbionts (FLE) [66] and *Rickettsia* [67]. Additionally, ticks can occasionally harbor other symbionts, such as *Wolbachia* [68] and *Arsenophonus* [69], which are less commonly found in ticks. Experimental evidence demonstrates vertically transmitted symbiont's protective role against pathogens or predators. Notably, studies show that antibiotics targeting *Coxiella*-LE and *Rickettsia*-LE reduce their densities [70], potentially affecting host fitness. This is exemplified in *H. longicornis*, where tetracycline treatment reduced *Coxiella*-LE levels, affecting the tick's fitness [70]. Additionally, the obligate *Coxiella*-like symbiont has been shown to manipulate the reproduction of its host, *Amblyomma americanum* [71].

Despite varying assembly patterns, *Acinetobacter* contributed to the stability of the AT group following node removal. Recently, this genus has been identified in the microbiome of field collected *H. longicornis* larvae, nymphs, and adults, with a higher abundance in larvae [72]. Additionally, it was detected in the midgut microbiome of fed specimens collected in China, demonstrating that *Acinetobacter* can stably colonize the midgut of *H. longicornis* [73]. Known for its broad antibiotic resistance [74, 75], this genus monitors antibiotic resistance genes and underscores ticks' potential as pathogen reservoirs [70]. For instance, the pathogen *Acinetobacter baumannii* shows high antimicrobial resistance development and acquisition of new resistance determinants [70, 76, 77]. Its response to antibiotics under iron limitation and oxidative stress is of interest, given its ability to express resistance to a wide range of antibiotics used in human medicine [78, 79].

Furthermore, the analysis of keystone taxa identification in both the CT and AT groups revealed distinct compositions between the two groups. *Ammoniphilus*, *Noviherbaspirillum*, and others were prominent in the CT group, whereas *Methyloceanibacter*, *Lysobacter*, and others were notable in the AT group. This suggests a shift in the microbial ecosystem following antibiotic intervention. These findings are consistent with prior research highlighting the significant role of specific bacterial taxa in tick microbiota and their potential susceptibility to antibiotics [18] [46]. These disruptions in microbial community assembly and node centrality likely contribute to the reduced colonization resistance observed in the AT group, as the antibiotics compromise the integrity and stability of the microbial network, making it more susceptible to colonization by pathogens like *Babesia*. Integrating community structure with functional dynamics represents a fundamental pursuit in microbial ecology [80], necessitating the exploration of microbial co-occurrence patterns and the identification of keystone taxa essential for ecosystem processes. The intricate interplay elucidated in this study among antibiotic treatment, keystone taxa, and microbial community dynamics provides profound insights beyond diversity studies. These findings establish a scientific basis for potential interventions targeting the modulation of tick microbiota to mitigate tick-borne diseases [81].

Robustness against network perturbations

The concept of robustness, which refers to the resistance of a network, can be elucidated through percolation theory [82], offering insights into information flow among network nodes [30]. Prior studies have employed in silico node removal to evaluate microorganism influence on plant microbiota properties [83]. This approach validated as a tool for predicting ecosystem behavior [30], suggests network robustness as indicative of microbial community resilience in diverse animal species, from arthropods [84, 46] to mammals [85]. This approach aims to induce infection-refractory states in ticks or other vectors [86, 87], ultimately reducing or blocking vector-borne pathogen transmission [88]. In this study, percolation theory was applied to evaluate network robustness by assessing loss in connectivity through degree, cascading, betweenness, and random attacks [30]. The results showed node removal had a more pronounced effect on both CT and AT networks compared to the random method, especially in the betweenness method. These findings suggest that while antibiotics administration can be discerned in the robustness test, its impact on bacterial community assembly appears limited compared to other disturbance factors [84]. This observation is consistent with previous research demonstrating a significant reduction in network robustness following directed attacks in the microbiota of mice exposed to antibiotics and fed a high-fat diet, as compared to untreated mice on the same diet [85]. From the result of this study, it can be proposed that specific antibiotics may target keystone taxa, potentially leading to ecosystem collapse [85]. The mechanisms by which antibiotics modulate the taxonomic and functional profiles of the tick microbiota are yet to be determined.

Functional implications

The analysis of predicted metabolic profiling of the microbiota was incorporated based on the novel bioinformatics tool PICRUSt2 [49]. Researching the effects of antibiotics on the functional characteristics of the microbiota of *H. longicornis* ticks has yielded some interesting results. In addition to changes in assembly patterns and community robustness, the functional profiles of microorganisms are affected as a consequence of antibiotic treatment. The AT had greater functional richness and evenness, implying broader metabolic capabilities compared to the CT group. This suggests that antibiotics may influence the metabolic diversity of the microbiota. Despite the existence of shared metabolic pathways, unique metabolic pathways were evident in both groups, denoting metabolic differences. Changes in the physicochemical properties of the ecosystem and the biological products that certain species produce may contribute to antibiotic resistance in other species [57]. Among the unique metabolic pathways in the AT group, the 2-heptyl-3-hydroxy-4(1H)-quinolone biosynthesis pathway was found. This molecule, known as the *Pseudomonas* quinolone signal (PQS), is important for its role in the quorum-sensing system that regulates biofilm formation, secondary metabolite production, pigment and virulence factor production, motility, and membrane vesicle formation [89]. Previous studies have revealed that exposure to subinhibitory concentrations of antibiotics induces the production of PQS in *Pseudomonas aeruginosa* [90]. Additionally, PQS has been shown to influence not only *P. aeruginosa* populations but also other bacterial species, regulating microbial communities within a specific ecosystem [91]. Therefore, in our study, antibiotic treatment may be triggering these cell-to-cell mechanisms to adapt and survive, facilitating the overgrowth of *Pseudomonas* species and other antibiotic-resistant bacteria. This could reduce the growth of beneficial endosymbionts species in the tick microbiome, which play an important role in tick metabolism and reproductive fitness [71, 92]. A disrupted microbiome could reduce tick's resistance to colonization of pathogens and other antibiotic-resistant bacteria, increasing the risk of transmitting diseases to the host. Furthermore, the proliferation of these bacteria species can potentially turn ticks into reservoirs and spreaders of antibiotic-resistant genes [93]. This underscores the importance of understanding the role of commensal organisms, such as *Coxiella*-like endosymbionts and *Acinetobacter* as significant metagenomic biomarkers [94]. For instance, the clinical significance of variances in antimicrobial susceptibility profiles among distinct genomic clusters of *Acinetobacter* has been elucidated [95], while the escalating recognition of efflux systems in facilitating multidrug resistance in *Acinetobacter* further underscores their critical role [96, 97].

Study limitations

This study has four major limitations: 1) Working with a small sample size may not capture the full spectrum of microbial diversity in both the AT and CT groups. Rare or less abundant microbial taxa might be underrepresented or missed, leading to an incomplete picture of the microbiome [98] and making the findings less robust for drawing definitive conclusions about the diversity and composition of the tick microbiome between both groups [99]. 2) Bacterial community structures vary significantly across tick life stages [100]. In some cases, the interaction pattern (co-occurrence or co-exclusion) changed according to the development stage [101]. For instance, higher bacterial diversity was observed in nymphal stages compared to adult stages of *Ixodes ricinus* ticks, likely due to distinct host-selection behaviors between immature and mature

ticks [100]. These variations can significantly impact how antibiotics affect the tick microbiota. 3) Our study utilized metagenomic data to characterize the functional profiles of the tick microbiota, focusing on potential genes and pathways present, but did not directly assess their active expression or functional significance under antibiotic exposure. Using richness and evenness metrics provide valuable insights into the diversity and distribution of functional pathways but may not fully capture functional redundancy, where different microbial species perform similar roles. This redundancy can mask changes in community composition without altering richness or evenness. This contrasts with meta-transcriptomics, which can provide direct insights into actively expressed genes by studying transcriptional regulation, metabolite dynamics, and protein signaling within tick microbial communities under antibiotic treatment. 4) Antibiotics targeting bacterial communities can disrupt microbial diversity and abundance, impacting microbiota-host interactions and potentially compromising the tick's ability to control pathogens [102]. These changes can also influence ecological niches, community stability, and interactions within the environment. Previous research has highlighted specific tick genes like longicin which is defensin-like protein of *H. longicornis* exerting anti-microbial and anti-fungal activity [103] and TROSPA, serum amyloid A, and calreticulin, which are implicated in vector-pathogen interactions during *Babesia* infection [104]. Further investigation into these biomarkers and proteins would enhance our understanding of how tick microbiota responds to antibiotics during *Babesia* infection, providing a better understanding of the tick immune response under antibiotics exposure and bring insights for optimizing treatment strategies against tick-borne diseases.

Conclusions

The current study provided a comprehensive exploration of the *H. longicornis* microbiota's response to antibiotic treatment, particularly in the context of *B. microti* transstadial transmission. The investigation into co-occurrence networks and keystone taxa showed the vulnerability of the tick microbiota to antibiotic-induced perturbations, observing notable differences in network centrality measures (degree, betweenness, closeness, and eigenvector centrality) and distinct keystone taxa compositions. Specifically, antibiotic treatment altered the clustering pattern of key taxa such as *Coxiella* and *Acinetobacter*, leading to a less robust microbial network and increased susceptibility to disturbance. Remarkably, the study uncovered novel insights into the functional consequences of antibiotic treatment, revealing increased functional richness and evenness in the antibiotic-treated group, implying broader metabolic capabilities and potential shifts in the importance of specific functions. These results suggest that antibiotic treatment can disrupt the microbial balance within ticks, decreasing their resistance to pathogen colonization. These findings carry broader ecological implications, emphasizing the need to consider functional aspects in understanding antibiotic-mediated reduction of colonization resistance and its implications for *Babesia* transstadial transmission. Our results offer a more detailed comprehension of tick microbiota dynamics under antibiotic treatment, revealing insights that were not evident through traditional assessments of bacterial diversity or abundance alone.

The intricate interplay between antibiotic treatment, microbial community dynamics, and functional profiles underscore the complexity of the tick microbiota, offering avenues for further research to manipulate these microbial communities for effective control of tick-borne diseases. In this context, anti-microbiota vaccines have been designed to modulate the tick microbiome by targeting essential microbial taxa [46, 105]. The use of co-occurrence networks and centrality measures to identify key taxa provides a robust method for developing these vaccines [105]. Anti-microbiota vaccines have been shown to effectively modulate the tick microbiome, impacting tick performance and pathogen colonization, thus supporting the development of this strategy for controlling tick-borne pathogens [106, 46, 107]. Additionally, alternative strategies in other vectors, such as paratransgenesis and phage therapy, have been explored to target specific taxa, which have demonstrated success in reducing pathogen load and vector competence [108, 109].

Supplementary Information

The online version contains supplementary material available at https://doi.org/10.1186/s12866-024-03468-1.

Supplementary Material 1: Supplementary Figure S1. Robustness comparison and node impact in the network's stability after removal of nodes between the CT and AT groups. Connectivity loss measured against directed (betweenness) and random attack: (A) CT/AT (betweenness) and (B) CT/AT (random). Connectivity loss measured against directed (betweenness) and random attack between the CT and AT networks after *Coxiella*' removal: (C) CT(woC)/AT(woC) (betweenness) and (D) CT(woC)/AT(woC) (random). Connectivity loss measured against directed and random attack between the CT and AT networks after *Acinetobacter*'s removal: (E) CT(woA)/AT (woA) (betweenness) and (F) CT(woA)/AT(woA) (random).

Supplementary Material 2: Supplementary Figure S2. Robustness comparison against removal of nodes in the presence and after taxa's removal within the same condition (CT or AT). Connectivity loss measured after directed (cascading) and random attack in *Coxiella*'s presence (wC) and removal (woC) between the same group: (A) CT (wC *vs.* woC), and (B) AT (wC *vs.* woC) in cascading, (C) CT (wC *vs.* woC), and (D) AT (wC *vs.* woC) in random. Connectivity loss measured after directed (cascading) and random attack in *Acinetobacter*'s presence (wA) and removal (woA) between the same group: (E) CT (wA *vs.* woA), and (F) AT (wA *vs.* woA) in cascading, (G) CT (wA *vs.* woA), and (H) AT (wA *vs.* woA) in random.

Supplementary Material 3: Supplementary Table S1. Taxa composition of *Coxiella* and *Acinetobacter*'s local connectivity in CT and AT groups.

Supplementary Material 4: Supplementary Table S2. Jaccard index for comparison between the same CT or AT group in presence and after *Coxiella*'s removal.

Supplementary Material 5: Supplementary Table S3. Jaccard index for comparison between the same CT or AT group in presence and after *Acinetobacter*'s removal.

Supplementary Material 6: Supplementary Table S4. Fraction of nodes removed to achieve 80% loss of connectivity between nodes in CT and AT networks and after removal of *Acinetobacter* (woA) and *Coxiella* (woC).

Supplementary Material 7: Supplementary Table S5. Largest connected component (LCC) and average path length (APL) values in the presence and after removal of *Coxiella* (wC/woC) and *Acinetobacter* (wA/woA) from the networks.

Supplementary Material 8: Supplementary Table S6. List of differential abundance of predicted metabolic pathways evaluated using the DESeq2 package and respective *p* values in CT and AT microbiota.

Supplementary Material 9: Supplementary Table S7. Shared and unique predicted bacterial pathways between the CT and AT microbiota.

Supplementary Material 10: Supplementary Table S8. Description of the unique metabolic pathways in the CT and AT groups.

Authors' contributions

Conceptualization: ACC, MK, EP-S. Formal analysis: MK, ALC-A, and EP-S. Investigation: MK, ICG, ALC-A, and EP-S. Resources: MBS, and ACC. Data Curation: LM-H. Writing—Original Draft: MK, EP-S, and ACC. Writing—Review & Editing: MK, AM, LA-D, EP-S, ICG, ALC-A, AW-C, TB, CA, JM, DO, LM-H, MBS, and ACC. Visualization: MK, and EP-S. Supervision: ACC.

Funding

UMR BIPAR is supported by the French Government's Investissement d'Avenir program, Laboratoire d'Excellence 'Integrative Biology of Emerging Infectious Diseases' (grant no. ANR-10-LABX-62-IBEID). ALC-A was supported by project "CLU-2019–05-IRNASA/CSIC Unit of Excellence", granted by the Junta de Castilla y León and co-financed by the European Union (ERDF).

Availability of data and materials

The datasets generated and analyzed during the current study are available in the National Center for Biotechnology Information's (NCBI) GenBank under Sequence Read Archive (SRA), deposited in accession numbers SRP322057 and SRP323180, https://www.ncbi.nlm.nih.gov/sra/?term=SRP322057.

Declarations

Ethics approval and consent to participate

Not applicable.

Consent for publication

Not applicable.

Competing interests

The authors declare no competing interests.

Author details

[1]Laboratory of Microbiology, National School of Veterinary Medicine of Sidi Thabet, University of Manouba, Manouba 2010, Tunisia. [2]UMR BIPAR, Laboratoire de Santé Animale, ANSES, INRAE, Ecole Nationale Vétérinaire d'Alfort, Maisons-Alfort 94700, France. [3]INRAE, UR 0045 Laboratoire de Recherches Sur Le Développement de L'Elevage (SELMET LRDE), Corte, France. [4]EA 7310, Laboratoire de Virologie, Université de Corse, Corte, France. [5]Animal Biotechnology Department, Center for Genetic Engineering and Biotechnology, P.O. Box 6162, Avenue 31 Between 158 and 190, Havana 10600, Cuba. [6]Direction of Animal Health, National Center for Animal and Plant Health, Carretera de Tapaste y Autopista Nacional, Apartado Postal 10, San José de Las Lajas, Mayabeque 32700, Cuba. [7]Immunology and Vaccines Laboratory, C. A. Facultad de Ciencias Naturales, Universidad Autónoma de Querétaro, Queretaro, Mexico. [8]C.A. Salud Animal y Microbiologia Ambiental. Facultad de Ciencias Naturales, Universidad Autonoma de Queretaro, Queretaro, Mexico. [9]Parasitology Laboratory, Institute of Natural Resources and Agrobiology (IRNASA, CSIC), Cordel de Merinas, 40-52, Salamanca 37008, Spain. [10]Department of Biological Sciences, Microbiology Unit, Kings University, Odeomu, Osun State, Nigeria. [11]National Agency for Food and Drug Control and Administration (NAFDAC), Isolo, Lagos State, Nigeria. [12]School of Environmental Sciences, University of Guelph, Guelph, ON, Canada. [13]Department of Basic Sciences, Higher Institute of Biotechnology of Sidi Thabet, University of Manouba, Manouba 2010, Tunisia.

Received: 7 May 2024 Accepted: 19 August 2024
Published online: 05 September 2024

References

1. Boulanger N, Boyer P, Talagrand-Reboul E, Hansmann Y. Ticks and tick-borne diseases. Med Mal Infect. 2019;49:87–97.
2. Jia N, Wang J, Shi W, Du L, Ye R-Z, Zhao F, et al. Haemaphysalis longicornis. Trends Genet. 2021;37:292–3.
3. Jiang J, An H, Lee JS, O'Guinn ML, Kim H-C, Chong S-T, et al. Molecular characterization of *Haemaphysalis longicornis*-borne rickettsiae, Republic of Korea and China. Ticks and Tick-borne Diseases. 2018;9:1606–13.
4. Zintl A, Mulcahy G, Skerrett HE, Taylor SM, Gray JS. *Babesia divergens*, a Bovine Blood Parasite of Veterinary and Zoonotic Importance. Clin Microbiol Rev. 2003;16:622–36.
5. Rizk MA, AbouLaila M, El-Sayed SA, Guswanto A, Yokoyama N, Igarashi I. Inhibitory effects of fluoroquinolone antibiotics on *Babesia divergens* and *Babesia microti*, blood parasites of veterinary and zoonotic importance. Infect Drug Resist. 2018;11:1605–15.
6. Yabsley MJ, Shock BC. Natural history of Zoonotic *Babesia*: Role of wildlife reservoirs. International Journal for Parasitology: Parasites and Wildlife. 2013;2:18–31.
7. Krause PJ. Human babesiosis. Int J Parasitol. 2019;49:165–74.
8. Schnittger L, Ganzinelli S, Bhoora R, Omondi D, Nijhof AM, Florin-Christensen M. The *Piroplasmida Babesia*, *Cytauxzoon*, and *Theileria* in farm and companion animals: species compilation, molecular phylogeny, and evolutionary insights. Parasitol Res. 2022;121:1207–45.
9. Ravindran R, Hembram PK, Kumar GS, Kumar KGA, Deepa CK, Varghese A. Transovarial transmission of pathogenic protozoa and rickettsial organisms in ticks. Parasitol Res. 2023;122:691–704.
10. Gray J, von Stedingk LV, Gürtelschmid M, Granström M. Transmission Studies of *Babesia microti* in *Ixodes ricinus* Ticks and Gerbils. J Clin Microbiol. 2002;40:1259–63.
11. Li L-H, Zhu D, Zhang C-C, Zhang Y, Zhou X-N. Experimental transmission of *Babesia microti* by *Rhipicephalus haemaphysaloides*. Parasit Vectors. 2016;9:231.
12. Yao J-M, Zhang H-B, Liu C-S, Tao Y, Yin M. Inhibitory effects of 19 antiprotozoal drugs and antibiotics on *Babesia microti* infection in BALB/c mice. J Infect Dev Ctries. 2015;9:1004–10.
13. Narasimhan S, Swei A, Abouneameh S, Pal U, Pedra JHF, Fikrig E. Grappling with the tick microbiome. Trends Parasitol. 2021;37:722–33.
14. Hussain S, Perveen N, Hussain A, Song B, Aziz MU, Zeb J, et al. The Symbiotic Continuum Within Ticks: Opportunities for Disease Control. Front Microbiol. 2022;13:854803.
15. Narasimhan S, Rajeevan N, Liu L, Zhao Yang O, Heisig J, Pan J, et al. Gut Microbiota of the Tick Vector *Ixodes scapularis* Modulate Colonization of the Lyme Disease Spirochete. Cell Host Microbe. 2014;15:58–71.
16. Wei N, Cao J, Zhang H, Zhou Y, Zhou J. The Tick Microbiota Dysbiosis Promote Tick-Borne Pathogen Transstadial Transmission in a *Babesia microti*–Infected Mouse Model. Front Cell Infect Microbiol. 2021;11:713466.
17. Gendrin M, Rodgers FH, Yerbanga RS, Ouédraogo JB, Basáñez M-G, Cohuet A, et al. Antibiotics in ingested human blood affect the mosquito microbiota and capacity to transmit malaria. Nat Commun. 2015;6(1):5921.
18. Wu-Chuang A, Hodžić A, Mateos-Hernández L, Estrada-Peña A, Obregon D, Cabezas-Cruz A. Current debates and advances in tick microbiome research. Curr Res Parasitol Vector-Borne Dis. 2021;1:100036.
19. Abuin-Denis L, Piloto-Sardiñas E, Maître A, Wu-Chuang A, Mateos-Hernández L, Obregon D, Corona-González B, Fogaça AC, Palinauskas

V, Aželytė J, Rodríguez-Mallon A, Cabezas-Cruz A. Exploring the impact of *Anaplasma phagocytophilum* on colonization resistance of Ixodes scapularis microbiota using network node manipulation. Curr Res Parasitol Vector Borne Dis. 2024;5:100177.
20. Jump RLP, Polinkovsky A, Hurless K, Sitzlar B, Eckart K, Tomas M, et al. Metabolomics Analysis Identifies Intestinal Microbiota-Derived Biomarkers of Colonization Resistance in Clindamycin-Treated Mice. PLoS ONE. 2014;9:e101267.
21. Mullineaux-Sanders C, Suez J, Elinav E, Frankel G. Sieving through gut models of colonization resistance. Nat Microbiol. 2018;3:132–40.
22. Ducarmon QR, Zwittink RD, Hornung BVH, van Schaik W, Young VB, Kuijper EJ. Gut Microbiota and Colonization Resistance against Bacterial Enteric Infection. Microbiol Mol Biol Rev. 2019;83(3):e00007-19.
23. Stacy A, Andrade-Oliveira V, McCulloch JA, Hild B, Oh JH, Perez-Chaparro PJ, et al. Infection trains the host for microbiota-enhanced resistance to pathogens. Cell. 2021;184:615-627.e17.
24. Karita Y, Limmer DT, Hallatschek O. Scale-dependent tipping points of bacterial colonization resistance. Proc Natl Acad Sci USA. 2022;119(7):e2115496119.
25. Spragge F, Bakkeren E, Jahn MT, Araújo E, Pearson C, Wang X, et al. Microbiome diversity protects against pathogens by nutrient blocking. Science. 2023;382(6676):eadj3502.
26. Levy R, Borenstein E. Metabolic modeling of species interaction in the human microbiome elucidates community-level assembly rules. Proc Natl Acad Sci. 2013;110:12804–9.
27. Shaw GTW, Liu AC, Weng CY, Chen YC, Chen CY, Weng FCH, et al. A network-based approach to deciphering a dynamic microbiome's response to a subtle perturbation. Sci Rep. 2020;10(1):19530.
28. Paerl HW, Dyble J, Moisander PH, Noble RT, Piehler MF, Pinckney JL, et al. Microbial indicators of aquatic ecosystem change: current applications to eutrophication studies. FEMS Microbiol Ecol. 2003;46:233–46.
29. Maitre A, Wu-Chuang A, Mateos-Hernández L, Piloto-Sardiñas E, Foucault-Simonin A, Cicculli V, et al. Rickettsial pathogens drive microbiota assembly in *Hyalomma marginatum and Rhipicephalus bursa ticks*. Mol Ecol. 2023;32:4660–76.
30. Röttjers L, Faust K. From hairballs to hypotheses–biological insights from microbial networks. FEMS Microbiol Rev. 2018;42:761–80.
31. Piloto-Sardiñas E, Abuin-Denis L, Maitre A, Foucault-Simonin A, Corona-González B, Díaz-Corona C, et al. Dynamic nesting of Anaplasma marginale in the microbial communities of Rhipicephalus microplus. Ecol Evol. 2024;14(4):e11228.
32. Bolyen E, Rideout JR, Dillon MR, Bokulich NA, Abnet CC, Al-Ghalith GA, et al. Reproducible, interactive, scalable and extensible microbiome data science using QIIME 2. Nat Biotechnol. 2019;37:852–7.
33. Callahan BJ, McMurdie PJ, Rosen MJ, Han AW, Johnson AJA, Holmes SP. DADA2: High-resolution sample inference from Illumina amplicon data. Nat Methods. 2016;13:581–3.
34. Yarza P, Yilmaz P, Pruesse E, Glöckner FO, Ludwig W, Schleifer K-H, et al. Uniting the classification of cultured and uncultured bacteria and archaea using 16S rRNA gene sequences. Nat Rev Microbiol. 2014;12:635–45.
35. Friedman J, Alm EJ. Inferring Correlation Networks from Genomic Survey Data. PLoS Comput Biol. 2012;8:e1002687.
36. Kurtz ZD, Müller CL, Miraldi ER, Littman DR, Blaser MJ, Bonneau RA. Sparse and Compositionally Robust Inference of Microbial Ecological Networks. PLoS Comput Biol. 2015;11:e1004226.
37. Bastian M, Heymann S, Jacomy M. Gephi: an open source software for exploring and manipulating networks. Third International AAAI Conference on Weblogs and Social Media. Vol. 3. 2009. https://ojs.aaai.org/index.php/ICWSM/article/view/13937.
38. Röttjers L, Vandeputte D, Raes J, Faust K. Null-model-based network comparison reveals core associations. ISME Commun. 2021;1:36.
39. Peschel S, Müller CL, von Mutius E, Boulesteix AL, Depner M. NetCoMi: network construction and comparison for microbiome data in R. Brief Bioinform. 2020;22(4):bbaa290.
40. R Core Team, 2023. R: A language and environment for statistical computing. R Foundation for Statistical Computing, Vienna, Austria. https://www.R-project.org/.
41. RStudio Team, 2020. RStudio: Integrated development for R. RStudio, PBC, Boston, MA, USA. http://www.rstudio.org/.
42. Real R, Vargas JM. The Probabilistic Basis of Jaccard's Index of Similarity. Syst Biol. 1996;45:380–5.
43. Guimerà R, Nunes Amaral LA. Functional cartography of complex metabolic networks. Nature. 2005;433:895–900.
44. Cao X, Zhao D, Xu H, Huang R, Zeng J, Yu Z. Heterogeneity of interactions of microbial communities in regions of Taihu Lake with different nutrient loadings: A network analysis. Sci Rep. 2018;8(1):8890.
45. Guo B, Zhang L, Sun H, Gao M, Yu N, Zhang Q, et al. Microbial co-occurrence network topological properties link with reactor parameters and reveal importance of low-abundance genera. NPJ Biofilms Microbiomes. 2022;8(1):3.
46. Mateos-Hernández L, Obregón D, Wu-Chuang A, Maye J, Bornères J, Versillé N, et al. Anti-Microbiota Vaccines Modulate the Tick Microbiome in a Taxon-Specific Manner. Front Immunol. 2021;12:704621.
47. Lhomme S. Analyse spatiale de la structure des réseaux techniques dans un contexte de risques. Cybergeo. 2015. https://doi.org/10.4000/cybergeo.26763.
48. Freitas VLS, Moreira GJP, Santos LBL. Robustness analysis in an inter-cities mobility network: modeling municipal, state and federal initiatives as failures and attacks toward SARS-CoV-2 containment. PeerJ. 2020;8:e10287-7.
49. Douglas GM, Maffei VJ, Zaneveld JR, Yurgel SN, Brown JR, Taylor CM, et al. PICRUSt2 for prediction of metagenome functions. Nat Biotechnol. 2020;38:685–8.
50. Kanehisa M, Goto S. KEGG: Kyoto Encyclopedia of Genes and Genomes. Nucleic Acids Res. 2000;28:27–30.
51. Caspi R, Billington R, Keseler IM, Kothari A, Krummenacker M, Midford PE, et al. The MetaCyc database of metabolic pathways and enzymes - a 2019 update. Nucleic Acids Res. 2019. https://doi.org/10.1093/nar/gkz862.
52. DeSantis TZ, Hugenholtz P, Larsen N, Rojas M, Brodie EL, Keller K, et al. Greengenes, a Chimera-Checked 16S rRNA Gene Database and Workbench Compatible with ARB. Appl Environ Microbiol. 2006;72:5069–72.
53. Pielou EC. The measurement of diversity in different types of biological collections. J Theor Biol. 1966;13:131–44.
54. Love MI, Huber W, Anders S. Moderated estimation of fold change and dispersion for RNA-seq data with DESeq2. Genome Biol. 2014;15:55.
55. Khan I, Bai Y, Zha L, Ullah N, Ullah H, Shah SRH, et al. Mechanism of the Gut Microbiota Colonization Resistance and Enteric Pathogen Infection. Front Cell Infect Microbiol. 2021;11:716299.
56. Schneider DS, Chambers MC. Rogue Insect Immunity. Science. 2008;322:1199–200.
57. Brownlie JC, Johnson KN. Symbiont-mediated protection in insect hosts. Trends Microbiol. 2009;17:348–54.
58. Nemergut DR, Schmidt SK, Fukami T, O'Neill SP, Bilinski TM, Stanish LF, et al. Patterns and Processes of Microbial Community Assembly. Microbiol Mol Biol Rev. 2013;77:342–56.
59. Bottery MJ, Matthews JL, Wood AJ, Johansen HK, Pitchford JW, Friman V-P. Inter-species interactions alter antibiotic efficacy in bacterial communities. ISME J. 2021;16(3):812–21.
60. de Vos MGJ, Zagórski M, McNally A, Bollenbach T. Interaction networks, ecological stability, and collective antibiotic tolerance in polymicrobial infections. Proc Natl Acad Sci USA. 2017;114:10666–71.
61. Aranda-Díaz A, Obadia B, Dodge R, Thomsen T, Hallberg ZF, Güvener ZT, et al. Bacterial interspecies interactions modulate pH-mediated antibiotic tolerance. eLife. 2020;9:e51493.
62. Vega NM, Gore J. Collective antibiotic resistance: mechanisms and implications. Curr Opin Microbiol. 2014;21:28–34.
63. Fogaça AC, Sousa G, Pavanelo DB, Esteves E, Martins LA, Urbanová V, et al. Tick Immune System: What Is Known, the Interconnections, the Gaps, and the Challenges. Front Immunol. 2021;12:628054.
64. Smith CA, Ashby B. Tolerance-conferring defensive symbionts and the evolution of parasite virulence. Evolution letters. 2023;7:262–72.
65. Almeida AP, Marcili A, Leite RC, Nieri-Bastos FA, Domingues LN, Martins JR, et al. *Coxiella* symbiont in the tick *Ornithodoros rostratus* (Acari: Argasidae). Ticks and Tick-Borne Diseases. 2012;3:203–6.
66. Ivanov IN, Mitkova N, Reye AL, Hübschen JM, Vatcheva-Dobrevska RS, Dobreva E, et al. Detection of New *Francisella*-Like Tick Endosymbionts in *Hyalomma* spp. and *Rhipicephalus* spp. (Acari: Ixodidae) from Bulgaria. Appl Environ Microbiol. 2011;77:5562–5.
67. Gillespie JJ, Joardar V, Williams KP, Driscoll T, Hostetler JB, Nordberg E, et al. A *Rickettsia* Genome Overrun by Mobile Genetic Elements Provides Insight into the Acquisition of Genes Characteristic of an Obligate Intracellular Lifestyle. J Bacteriol. 2012;194:376–94.

68. Zhang X, Norris DE, Rasgon JL. Distribution and molecular characterization of *Wolbachia* endosymbionts and filarial nematodes in Maryland populations of the lone star tick (*Amblyomma americanum*). FEMS Microbiol Ecol. 2011;77:50–6.
69. Dergousoff SJ, Chilton NB. Detection of a new *Arsenophonus*-type bacterium in Canadian populations of the Rocky Mountain wood tick. Dermacentor andersoni Experimental and Applied Acarology. 2010;52:85–91.
70. Zhang C-M, Li N-X, Zhang T-T, Qiu Z-X, Li Y, Li L-W, et al. Endosymbiont CLS-HI plays a role in reproduction and development of *Haemaphysalis longicornis*. Exp Appl Acarol. 2017;73:429–38.
71. Zhong J, Jasinskas A, Barbour AG. Antibiotic Treatment of the Tick Vector *Amblyomma americanum* Reduced Reproductive Fitness. PLoS ONE. 2007;2:e405.
72. Ponnusamy L, Travanty NV, Watson DW, Seagle SW, Boyce RM, Reiskind MH. Microbiome of Invasive Tick Species *Haemaphysalis Longicornis* in North Carolina. USA Insects. 2024;15:153.
73. Liu Z-L, Qiu Q-G, Cheng T-Y, Liu G-H, Liu L, Duan D-Y. Composition of the Midgut Microbiota Structure of *Haemaphysalis longicornis* Tick Parasitizing Tiger and Deer. Animals. 2024;14:1557–67.
74. Shin B, Park W. Antibiotic resistance of pathogenic *Acinetobacter* species and emerging combination therapy. J Microbiol. 2017;55:837–49.
75. Wei N, Lu J, Dong Y, Li S. Profiles of Microbial Community and Antibiotic Resistome in Wild Tick Species. mSystems. 2022;7(4):e0003722.
76. Poirel L, Bonnin RA, Nordmann P. Genetic basis of antibiotic resistance in pathogenic *Acinetobacter* species. IUBMB Life. 2011;63:1061–7.
77. Vrancianu CO, Gheorghe I, Czobor IB, Chifiriuc MC. Antibiotic Resistance Profiles, Molecular Mechanisms and Innovative Treatment Strategies of *Acinetobacter baumannii*. Microorganisms. 2020;8:935.
78. Garnacho-Montero J, Amaya-Villar R. Multiresistant *Acinetobacter baumannii* infections: epidemiology and management. Curr Opin Infect Dis. 2010;23:332–9.
79. Fiester SE, Actis LA. Stress responses in the opportunistic pathogen *Acinetobacter baumannii*. Future Microbiol. 2013;8:353–65.
80. Prosser JI, Bohannan BJM, Curtis TP, Ellis RJ, Firestone MK, Freckleton RP, et al. The role of ecological theory in microbial ecology. Nat Rev Microbiol. 2007;5:384–92.
81. Banerjee S, Schlaeppi K, van der Heijden MGA. Keystone taxa as drivers of microbiome structure and functioning. Nat Rev Microbiol. 2018;16:567–76.
82. Cohen R, Erez K, ben-Avraham D, Havlin S. Resilience of the Internet to Random Breakdowns. Phys Rev Lett. 2000;85:4626–8.
83. Agler MT, Ruhe J, Kroll S, Morhenn C, Kim S-T, Weigel D, et al. Microbial Hub Taxa Link Host and Abiotic Factors to Plant Microbiome Variation. PLoS Biol. 2016;14:e1002352.
84. Estrada-Peña A, Cabezas-Cruz A, Obregón D. Resistance of Tick Gut Microbiome to Anti-Tick Vaccines. Pathogen Infection and Antimicrobial Peptides Pathogens. 2020;9:309.
85. Mahana D, Trent CM, Kurtz ZD, Bokulich NA, Battaglia T, Chung J, et al. Antibiotic perturbation of the murine gut microbiome enhances the adiposity, insulin resistance, and liver disease associated with high-fat diet. Genome Med. 2016;8(1):48.
86. Maitre A, Wu-Chuang A, Aželytė J, Palinauskas V, Mateos-Hernández L, Obregon D, et al. Vector microbiota manipulation by host antibodies: the forgotten strategy to develop transmission-blocking vaccines. Parasit Vectors. 2022;15(1):4.
87. Maitre A, Wu-Chuang A, Mateos-Hernández L, Foucault-Simonin A, Moutailler S, Paoli J-C, et al. *Rickettsia helvetica* infection is associated with microbiome modulation in *Ixodes ricinus* collected from humans in Serbia. Sci Rep. 2022;12:11464.
88. Aželytė J, Wu-Chuang A, Žiegytė R, Platonova E, Mateos-Hernandez L, Maye J, et al. Anti-Microbiota Vaccine Reduces Avian Malaria Infection Within Mosquito Vectors. Front Immunol. 2022;13:841835.
89. Reen FJ, Mooij MJ, Holcombe LJ, McSweeney CM, McGlacken GP, Morrissey JP, et al. The *Pseudomonas* quinolone signal (PQS), and its precursor HHQ, modulate interspecies and interkingdom behaviour. FEMS Microbiol Ecol. 2011;77:413–28.
90. Cummins J, Reen FJ, Baysse C, Mooij MJ, O'Gara F. Subinhibitory concentrations of the cationic antimicrobial peptide colistin induce the pseudomonas quinolone signal in *Pseudomonas aeruginosa*. Microbiology. 2009;155:2826–37.
91. Toyofuku M, Nakajima-Kambe T, Uchiyama H, Nomura N. The Effect of a Cell-to-Cell Communication Molecule, Pseudomonas Quinolone Signal (PQS), Produced by *P. aeruginosa* on Other Bacterial Species. Microbes Environ. 2010;25:1–7.
92. Cibichakravarthy B, Shaked N, Kapri E, Gottlieb Y. Endosymbiont-derived metabolites are essential for tick host reproductive fitness. mSphere. 2024;9(7):e00693-23. https://doi.org/10.1128/msphere.00693-23.
93. Chavarría-Bencomo IV, Nevárez-Moorillón GV, Espino-Solís GP, Adame-Gallegos JR. Antibiotic resistance in tick-borne bacteria: A One Health approach perspective. J Infect Public Health. 2023;16:153–62.
94. Chigwada AD, Mapholi NO, Ogola HJO, Mbizeni S, Masebe TM. Pathogenic and Endosymbiotic Bacteria and Their Associated Antibiotic Resistance Biomarkers in *Amblyomma* and *Hyalomma* Ticks Infesting Nguni Cattle (Bos spp.). Pathogens. 2022;11:432.
95. Houang ETS, Chu YW, Chu KY, Ng KC, Leung CM, Cheng AFB. Significance of Genomic DNA Group Delineation in Comparative Studies of Antimicrobial Susceptibility of *Acinetobacter* spp. Antimicrob Agents Chemother. 2003;47:1472–5.
96. Coyne S, Courvalin P, Périchon B. Efflux-mediated antibiotic resistance in *Acinetobacter* spp. Antimicrob Agents Chemother. 2011;55:947–53.
97. Nikaido H, Pagès J-M. Broad-specificity efflux pumps and their role in multidrug resistance of Gram-negative bacteria. FEMS Microbiol Rev. 2012;36:340–63.
98. Chen Y, Fan L, Chai Y, Xu J. Advantages and challenges of metagenomic sequencing for the diagnosis of pulmonary infectious diseases. Clin Respir J. 2022;16:646–56.
99. National Research Council (US) Committee on Metagenomics: Challenges and Functional Applications. The New Science of Metagenomics: Revealing the Secrets of Our Microbial Planet. Washington (DC): National Academies Press (US); 2007. 4, Designing a Successful Metagenomics Project: Best Practices and Future Needs. Available from: https://www.ncbi.nlm.nih.gov/books/NBK54007/
100. Carpi G, Cagnacci F, Wittekindt NE, Zhao F, Qi J, Tomsho LP, et al. Metagenomic Profile of the Bacterial Communities Associated with *Ixodes ricinus Ticks*. PLoS ONE. 2011;6:e25604.
101. Gomard Y, Flores O, Vittecoq M, Blanchon T, Toty C, Duron O, et al. Changes in Bacterial Diversity, Composition and Interactions During the Development of the Seabird Tick Ornithodoros maritimus (Argasidae). Microb Ecol. 2020;81:770–83.
102. Hajdušek O, Šíma R, Ayllón N, Jalovecká M, Perner J, de la Fuente J, et al. Interaction of the tick immune system with transmitted pathogens. Front Cell Infect Microbiol. 2013;3:26.
103. Tsuji N, Fujisaki K. Longicin plays a crucial role in inhibiting the transmission of *Babesia* parasites in the vector tick *Haemaphysalis longicornis*. Future Microbiol. 2007;2:575–8.
104. Antunes S, Galindo RC, Almazán C, Rudenko N, Golovchenko M, Grubhoffer L, et al. Functional genomics studies of *Rhipicephalus* (*Boophilus*) *annulatus* ticks in response to infection with the cattle protozoan parasite, *Babesia bigemina*. Int J Parasitol. 2012;42:187–95.
105. Wu-Chuang A, Obregon D, Mateos-Hernández L, Cabezas-Cruz A. Anti-tick microbiota vaccines: how can this actually work? Biologia. 2021. https://doi.org/10.1007/s11756-021-00818-6.
106. Wu-Chuang A, Mateos-Hernández L, Maitre A, Rego RO, Šíma R, Porcelli S, et al. Microbiota perturbation by anti-microbiota vaccine reduces the colonization of *Borrelia afzelii in Ixodes ricinus*. Microbiome. 2023;11(1):151.
107. Mateos-Hernández L, Obregón D, Maye J, Borneres J, Versille N, de la Fuente J, et al. Anti-Tick Microbiota Vaccine Impacts *Ixodes ricinus* Performance during Feeding. Vaccines. 2020;8:702.
108. Tikhe CV, Dimopoulos G. Phage Therapy for Mosquito Larval Control: a Proof-of-Principle Study. mBio. 2022;13:e03017-22.
109. Fofana A, Yerbanga RS, Bilgo E, Ouedraogo GA, Gendrin M, Ouedraogo JB. The Strategy of Paratransgenesis for the Control of Malaria Transmission. Front Trop Dis. 2022;3:867104.

Publisher's Note